Supplementary Information For:

Ultrafast and nanomolar level detection of H_2S in water using a functionalized UiO-66 MOF based fluorescent chemosensor

*Subhrajyoti Ghosh and Shyam Biswas**

Department of Chemistry, Indian Institute of Technology Guwahati, Guwahati, 781039 Assam, India

*To whom correspondence should be addressed. E-mail: sbiswas@iitg.ac.in; Tel: 91-3612583309.

Materials and Characterization Methods:

The synthesis and characterisation procedures for 2-(nitrophenoxy)terepththalic acid (H_2BDC-O-Ph-NO_2) ligand are described below. All the chemicals were purchased from commercial sources and used without further purification. A Bruker Avance III 600 spectrometer was utilized for recording ^{1}H NMR and ^{13}C NMR spectra at 400 MHz and 100 MHz respectively. The mass spectrum (in ESI mode) was measured with an Agilent 6520 Q-TOF high-resolution mass spectrometer. Fourier transform infrared (FT-IR) spectroscopy data were recorded in the region 400-4000 cm^{-1} at room temperature with the Perkin Elmer Spectrum Two FT-IR spectrometer. The following indications were used to indicate the corresponding absorption bands: very strong (vs), strong (s), medium (m), weak (w), shoulder (sh) and broad (br). Thermogravimetric (TG) experiments were carried out with a heating rate of 10 °C min^{-1} under argon atmosphere using a SDT Q600 thermogravimetric analyser. Powder X-ray diffraction (PXRD) data were collected in transmission mode using a Bruker D2 Phaser X-ray diffractometer (30 kV, 10 mA) using Cu-*K*α (λ = 1.5406 Å) radiation. Specific surface area for N_2 sorption was calculated on a Quantachrome Autosorb iQMP gas sorption analyser at -196 °C. FE-SEM images were collected with a Zeiss (Sigma 300) scanning electron microscope. The compound was activated at 100 °C for 24 h under dynamic vacuum. Fluorescence emission studies were performed at room temperature using a HORIBA JOBIN YVON Fluoromax-4 spectrofluorometer.

Synthesis Procedure for H_2BDC-O-Ph-NO_2 Linker:

The synthesis of H_2BDC-O-Ph-NO_2 linker involves two elementary steps. Here, we used dimethyl-2-hydroxyterephthalate and 1-fluoro-4-nitrobenzene as the starting materials.

First step: In presence of 25 mL of dry *N,N*-dimethylacetamide, dimethyl-2-hydroxyterephthalate (500 mg, 2.38 mmol) and 1-fluoro-4-nitrobenzene (403 mg, 2.85 mmol) were mixed in a 50 mL round bottom flask, and 985 mg (7.14 mmol) K_2CO_3 was added portion wise to the mixture. After adding K_2CO_3, the reaction mixture was allowed to heat at 120 °C for 24 h under nitrogen atmosphere. After completion of 24 h, the reaction mixture was allowed to cool down to room temperature. The mixture was poured into an ice/water mixture and a white coloured precipitate was obtained. The precipitate was filtered and washed with cold water for few times. Finally, it was dried at 50 °C for 6 h inside an air oven. The dry compound was used in the second step. Yield: 655 mg (1.97 mmol, 83%).

Second step: The ester compound obtained in the first step was hydrolysed in this step. For this purpose, 500 mg (1.51 mmol) of the ester compound was taken in a 100 mL round bottom flask and 25 mL of THF, 25 mL of EtOH, 25 mL of 1 (M) LiOH solution were added to it. The mixture was heated at 60 °C for 3 h under stirring conditions. After 3 h, the solvents (THF and EtOH) were evaporated and rest of the solution was acidified using 3 (M) HCl solution. Finally, a white coloured precipitate was obtained, which was filtered under vacuum. The precipitate was dried at 50 °C for 24 h in an air oven. Yield: 430 mg (1.41 mmol, 94%). ^{1}H NMR (400 MHz, DMSO-d_6): δ = 8.24 (d, 2H), 8.04 (d, 2H), 7.92 (d, 1H),

7.66 (d, 1H), 7.08 (d,2H) ppm. ppm. ^{13}C NMR (100 MHz, DMSO-d_6): δ = 165.90, 165.50, 163.17, 152.83, 142.40, 136.09, 132.38, 129.04, 126.62, 126.24, 123.34, 117.15 ppm. ESI-MS (m/z): 302.1138 for $(M-H)^-$ ion (M = mass of H_2BDC-O-Ph-NO_2 linker). The NMR and mass spectra of the H_2BDC-O-Ph-NO_2 linker are shown in Figures S1-S3.

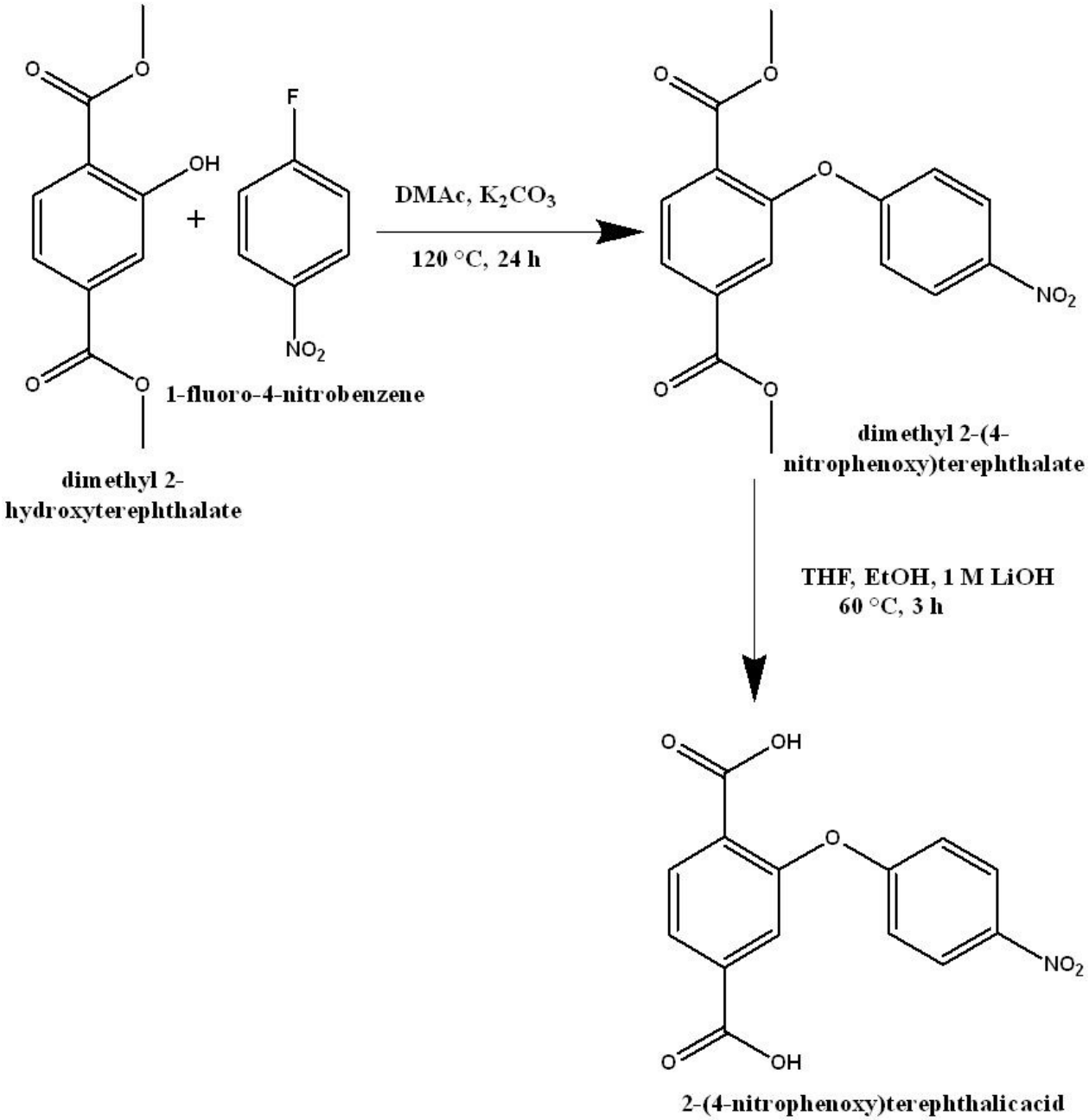

Scheme S1. Scheme of reactions for the preparation of H_2BDC-O-Ph-NO_2 linker.

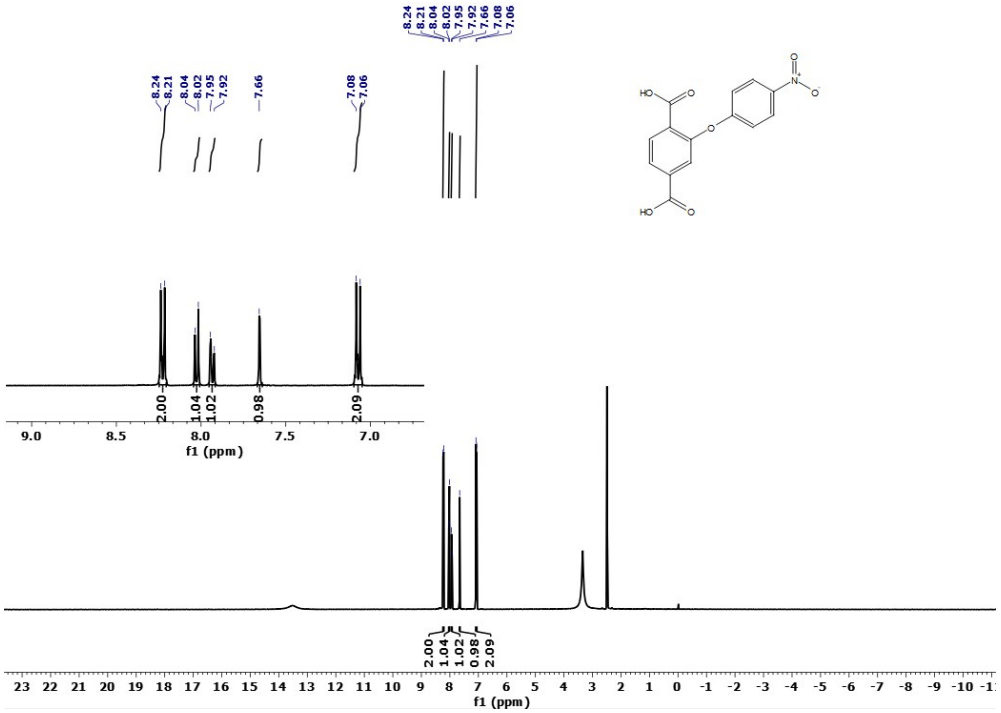

Figure S1. ^{1}H NMR spectrum of H_2BDC-O-Ph-NO_2 linker in DMSO-d_6.

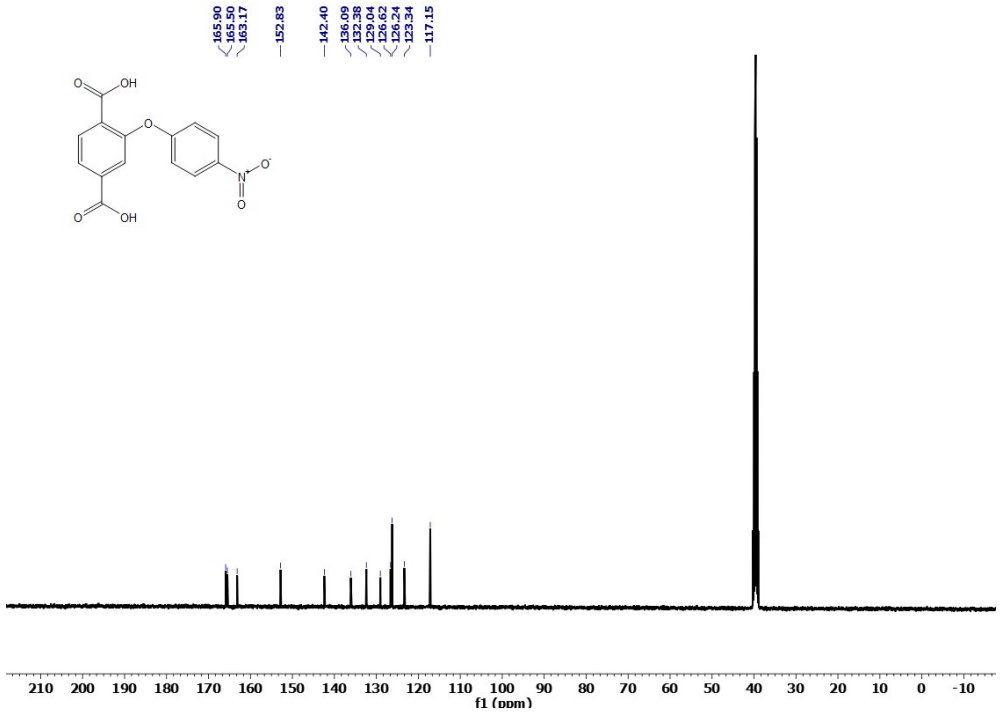

Figure S2. ^{13}C NMR spectrum of H_2BDC-O-Ph-NO_2 linker in DMSO-d_6.

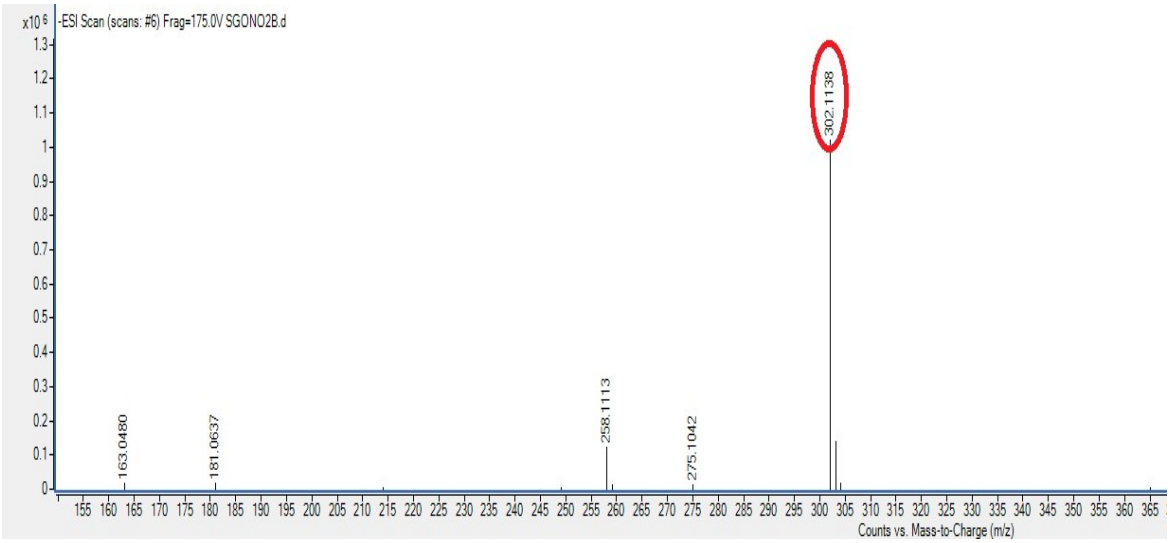

Figure S3. ESI-MS spectrum of H_2BDC-O-Ph-NO_2 linker measured in methanol. The spectrum shows m/z peak at 302.1138, which corresponds to $(M\text{-}H)^-$ ion (M = mass of H_2BDC-O-Ph-NO_2 linker).

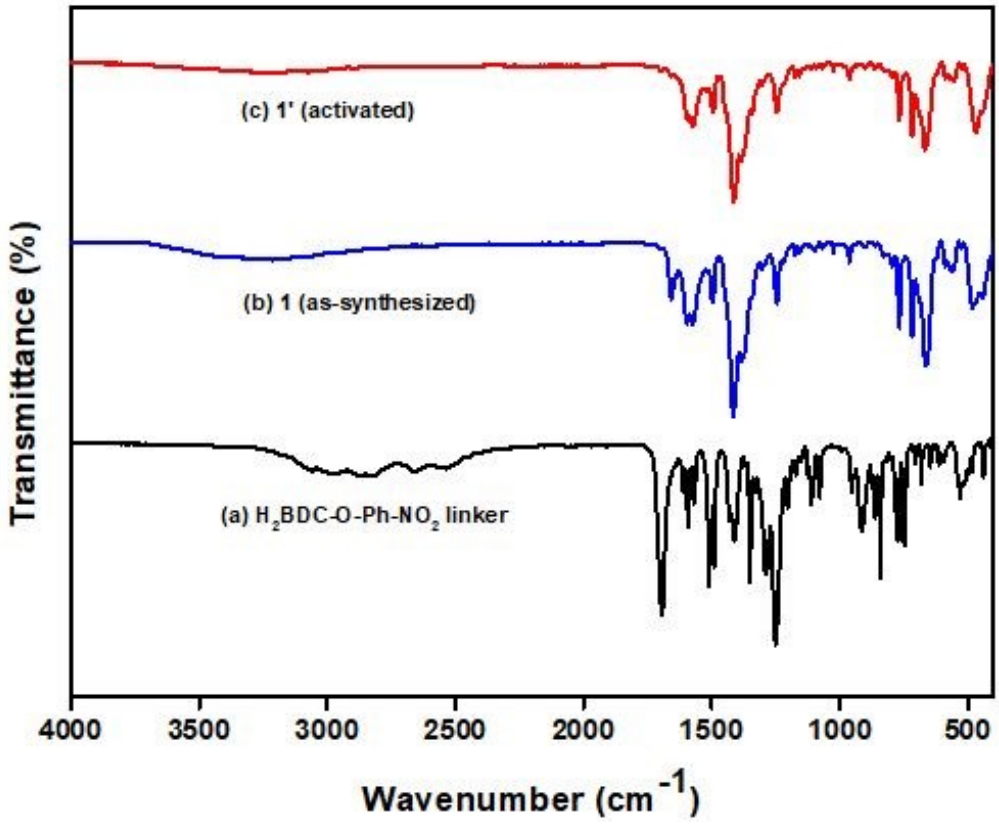

Figure S4. FT-IR spectra of (a) H_2BDC-O-Ph-NO_2 linker, (b) as-synthesized **1** and (c) activated **1′**

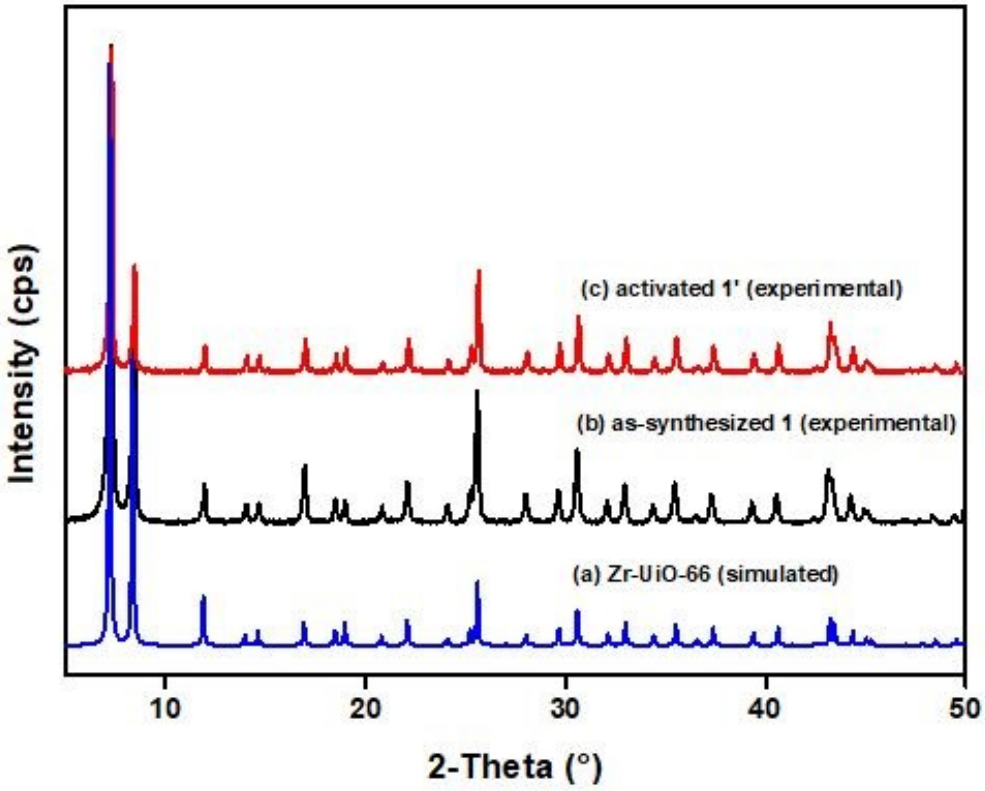

Figure S5. PXRD patterns of (a) Zr-UiO-66 (simulated), (b) as-synthesized **1** (black) and (c) activated **1′** (red).

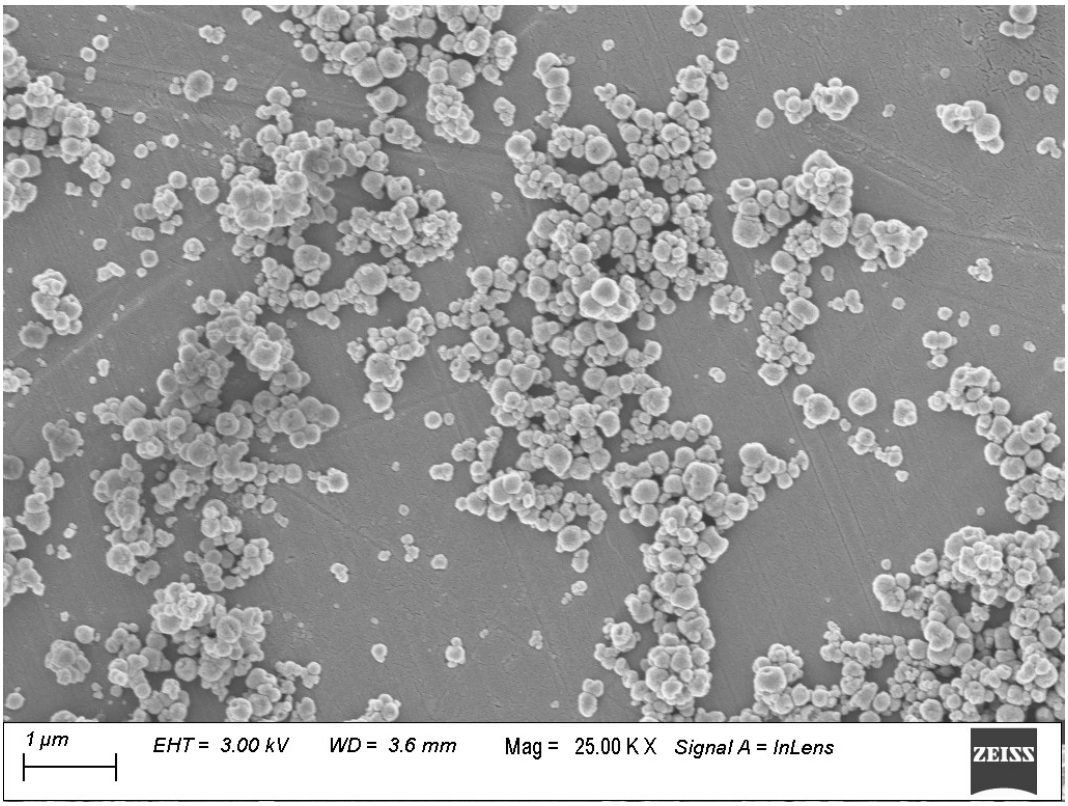

Figure S6. FE-SEM image of **1**.

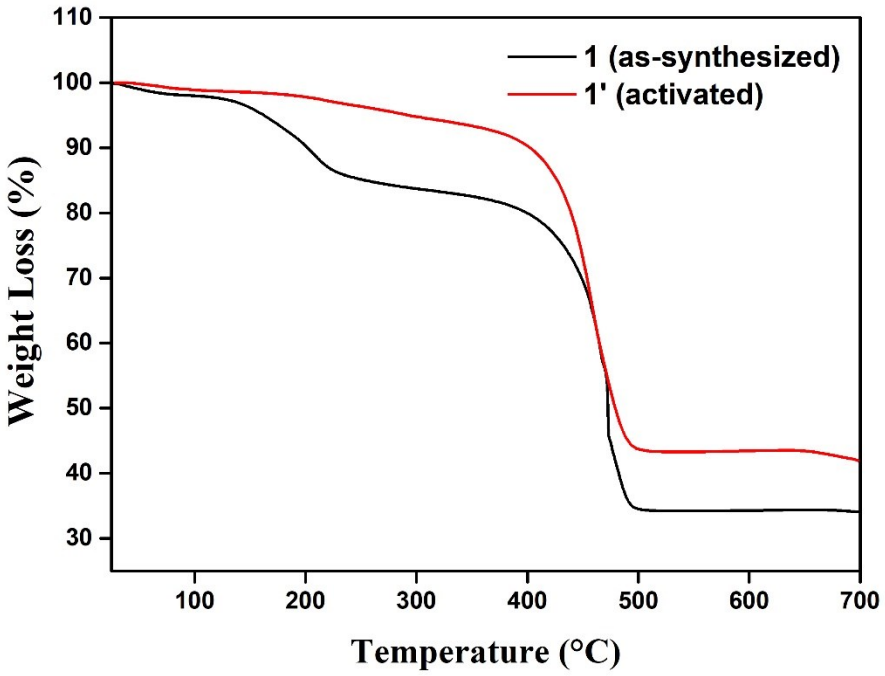

Figure S7. Thermogravimetric curves of as-synthesized **1** (black) and activated **1′** (red) recorded under argon atmosphere in the temperature range of 25-700 °C with a heating rate of 5 °C min^{-1}.

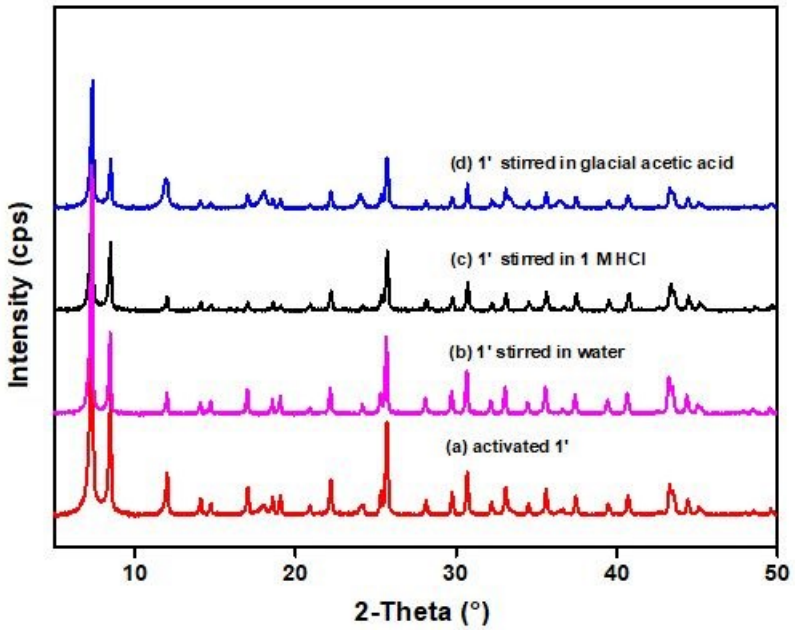

Figure S8. PXRD patterns of un-treated **1′** (a) and **1′** (b) after stirring in water for 24 h, (c) after stirring in 1 (M) HCl for 24 h and (d) after stirring in glacial acetic acid for 24 h.

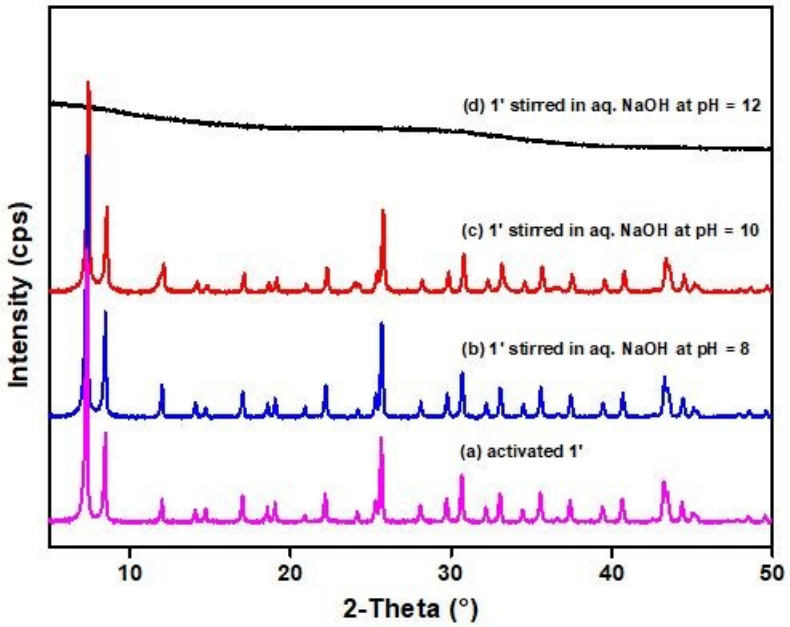

Figure S9. PXRD patterns of un-treated **1′** (a) and **1′** in aq. NaOH solutions having various pH values: (b) after stirring in aq. NaOH solution at pH = 8 for 4 h, (c) after stirring in aq. NaOH solution at pH = 10 for 4 h and (d) after stirring in aq. NaOH solution at pH = 12 for 4 h.

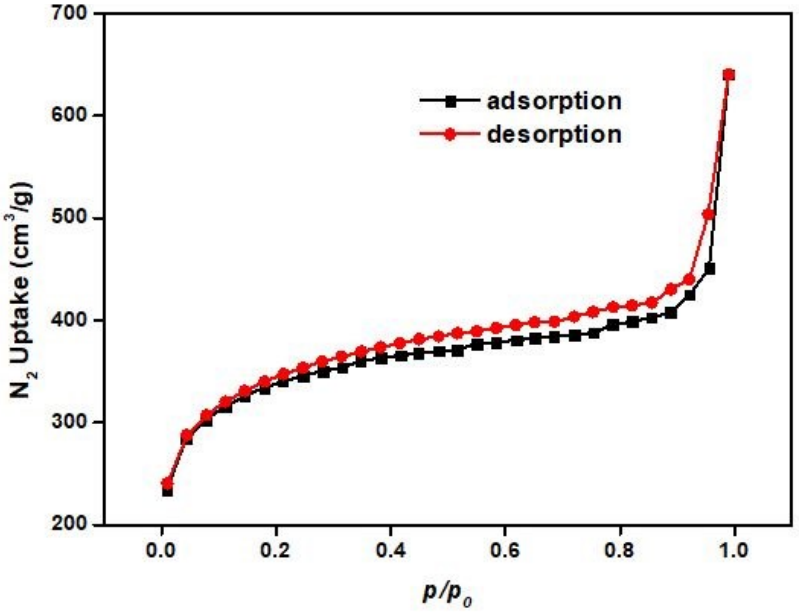

Figure S10. N_2 adsorption (black circles) and desorption (red circles) isotherms of thermally activated **1'** recorded at –196 °C.

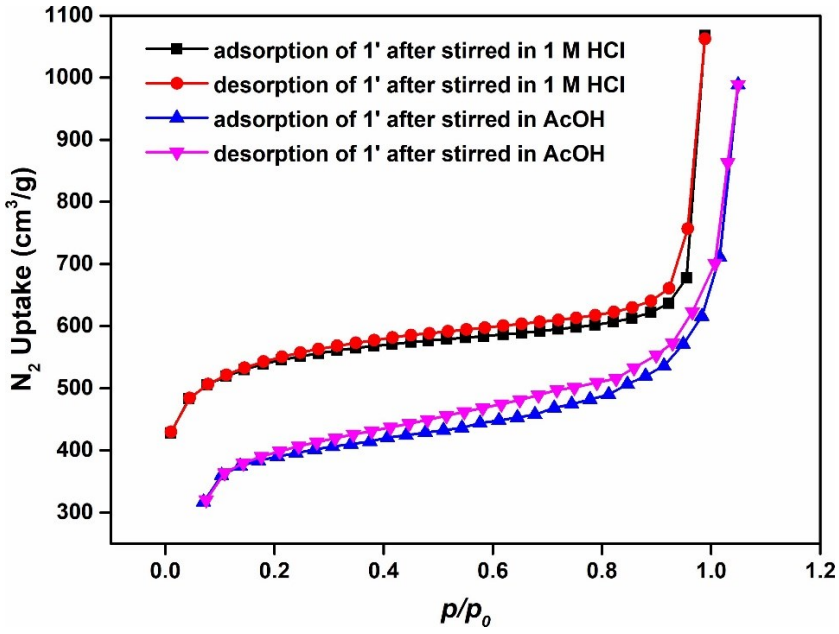

Figure S11. N_2 adsorption (black circles) and desorption (red circles) isotherms of thermally activated **1'** after 1 M HCl exchange, and N_2 adsorption (blue) and desorption (pink) isotherms of thermally activated **1'** after AcOH exchange recorded at –196 °C.

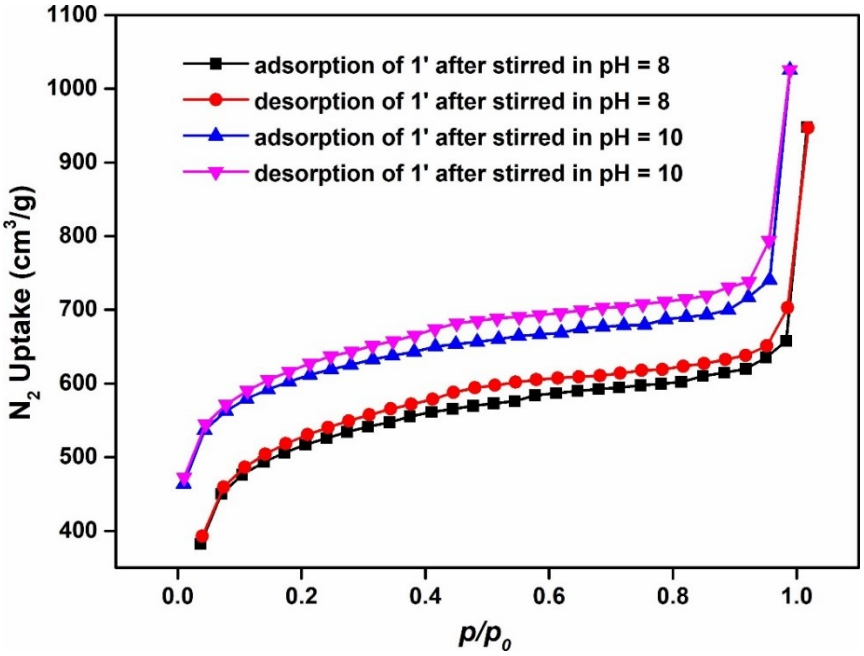

Figure S12. N_2 adsorption (black circles) and desorption (red circles) isotherms of thermally activated **1'** after exchange with NaOH at pH = 8 solution, and N_2 adsorption (blue) and desorption (pink) isotherms of thermally activated **1'** after exchange with NaOH at pH = 10 solution recorded at –196 °C.

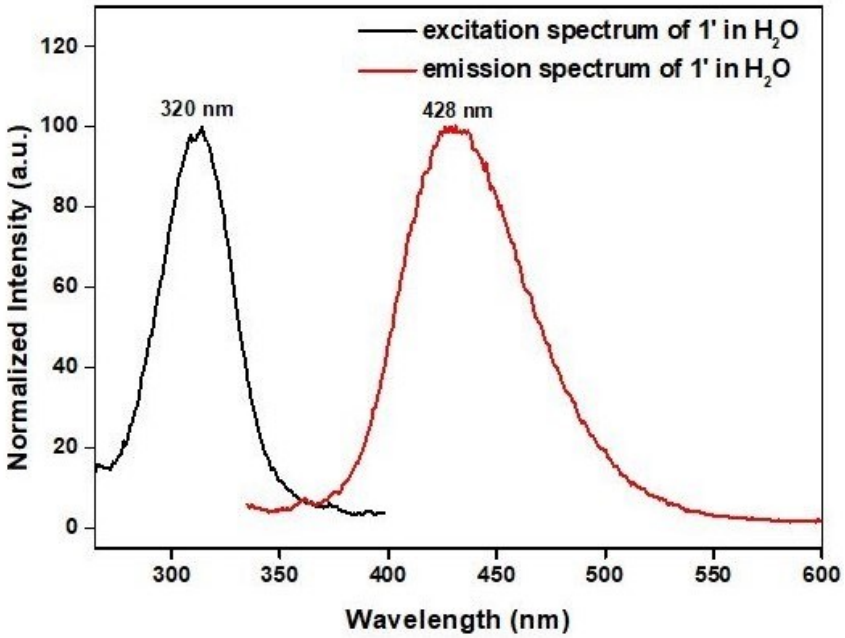

Figure S13. Excitation (black) and emission (red) spectra of **1′** in water.

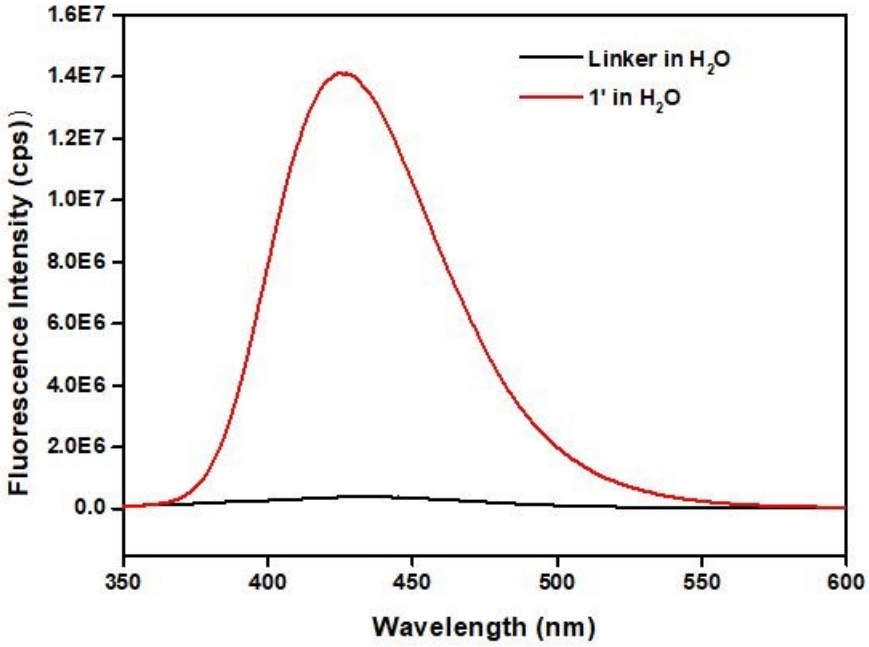

Figure S14. Luminescence spectra of free H_2BDC-O-Ph-NO_2 linker and **1′** in H_2O (λ_{ex} = 320 nm).

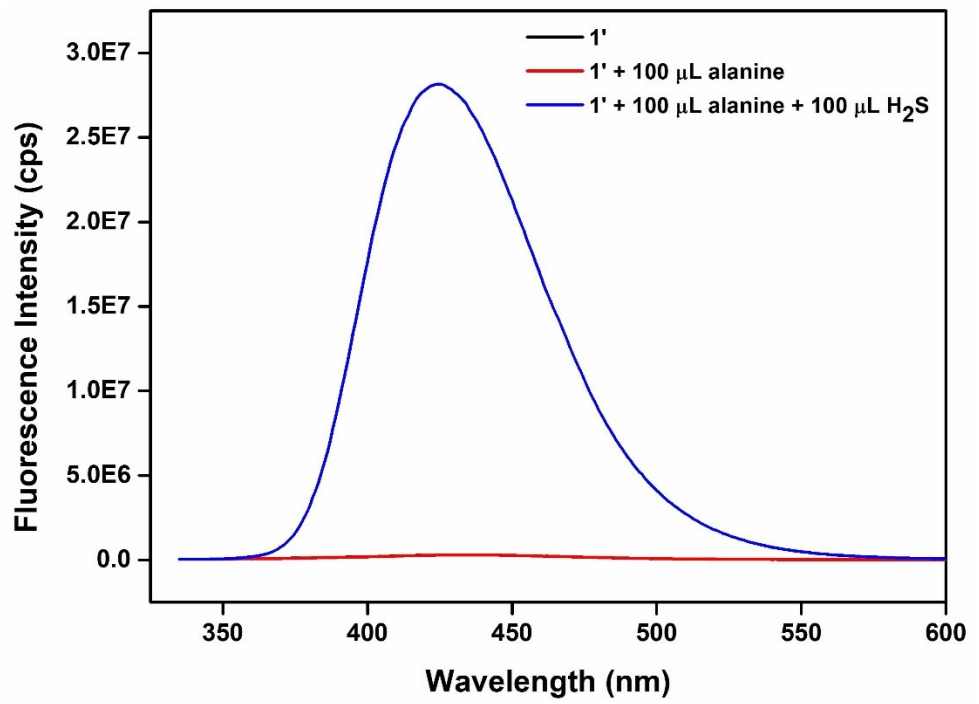

Figure S15. Switch-on fluorescence intensity of the aqueous solution of **1′** after addition of 100 μL of 10 mM aqueous Na_2S solution in presence of 100 μL of 10 mM aqueous solution of alanine.

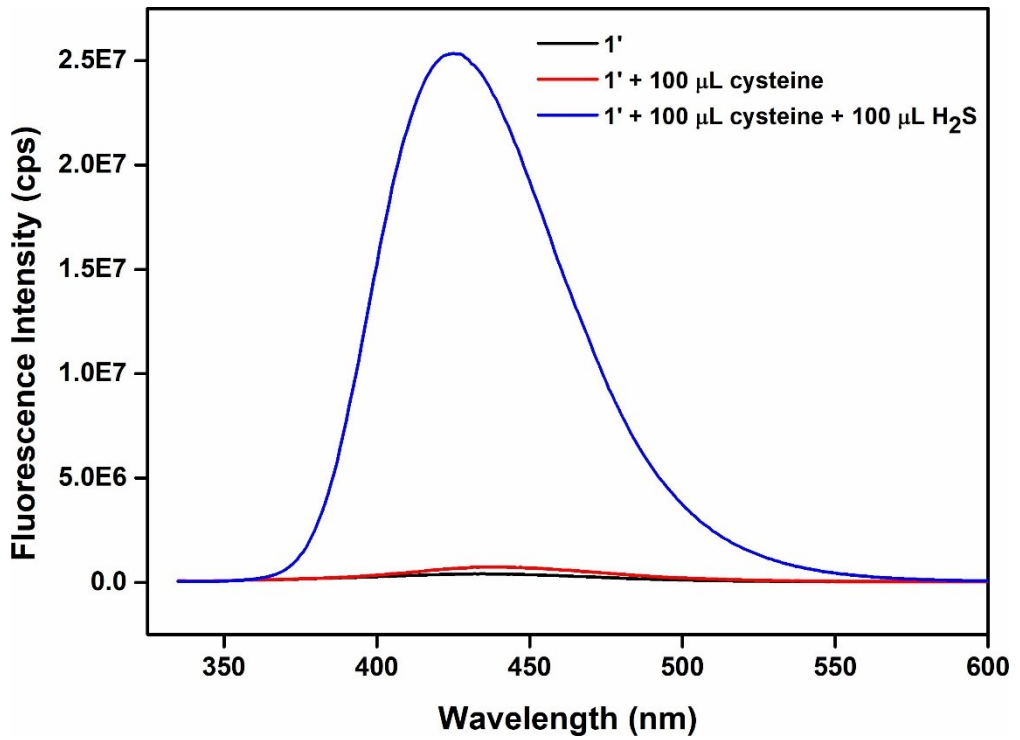

Figure S16. Switch-on fluorescence intensity of the aqueous solution of **1′** after addition of 100 μL of 10 mM aqueous Na_2S solution in presence of 100 μL of 10 mM aqueous solution of cysteine.

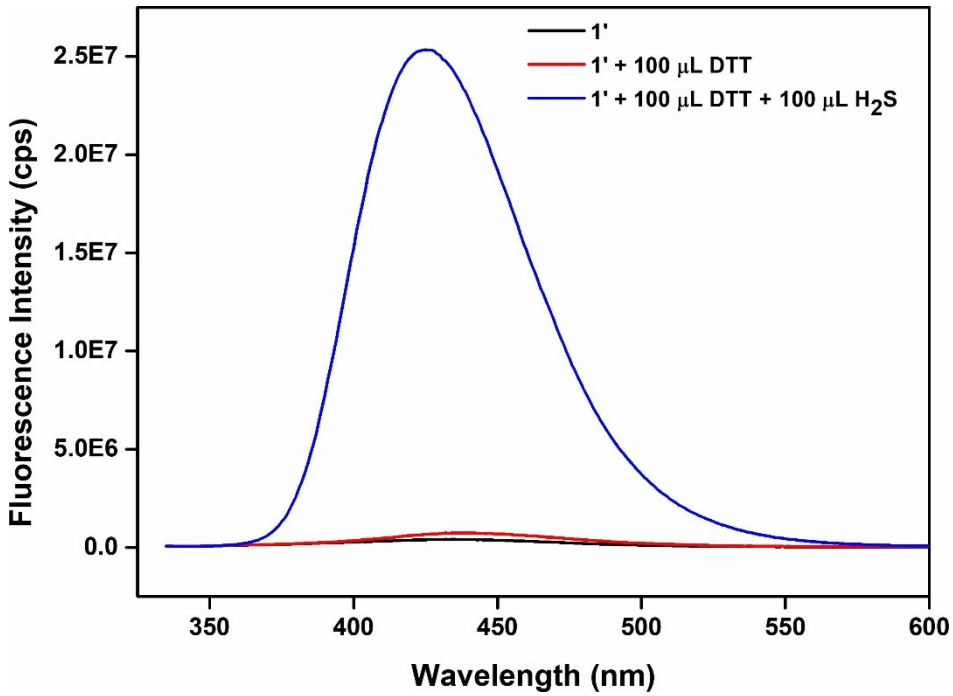

Figure S17. Switch-on fluorescence intensity of the aqueous solution of **1′** after addition of 100 μL of 10 mM aqueous Na_2S solution in presence of 100 μL of 10 mM aqueous solution of DTT.

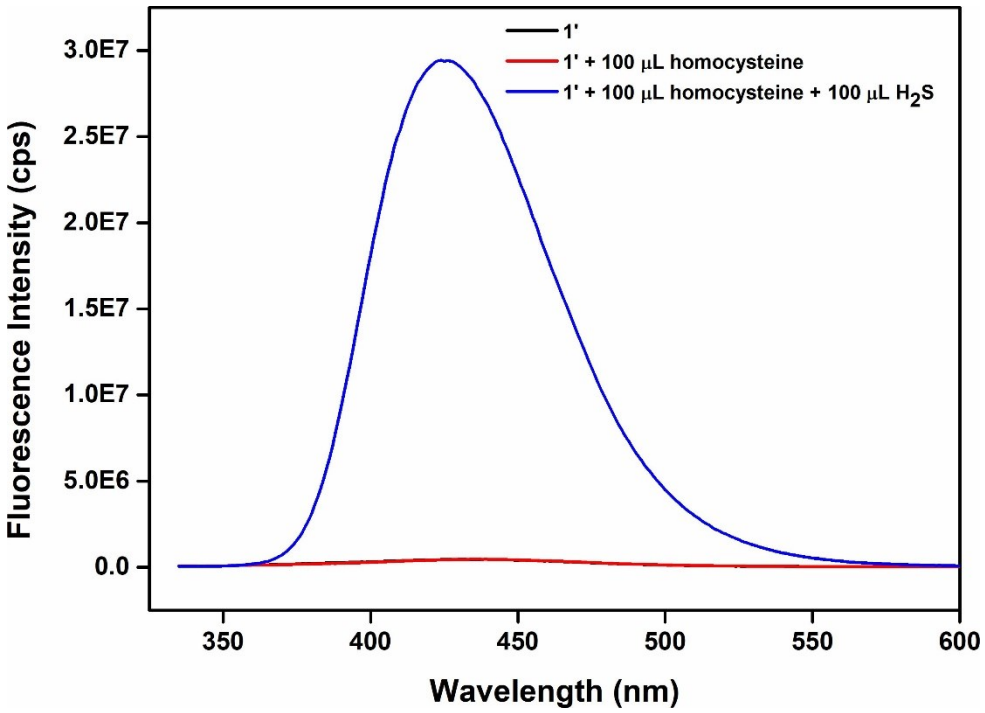

Figure S18. Switch-on fluorescence intensity of the aqueous solution of **1′** after addition of 100 μL of 10 mM aqueous Na_2S solution in presence of 100 μL of 10 mM aqueous solution of homocysteine.

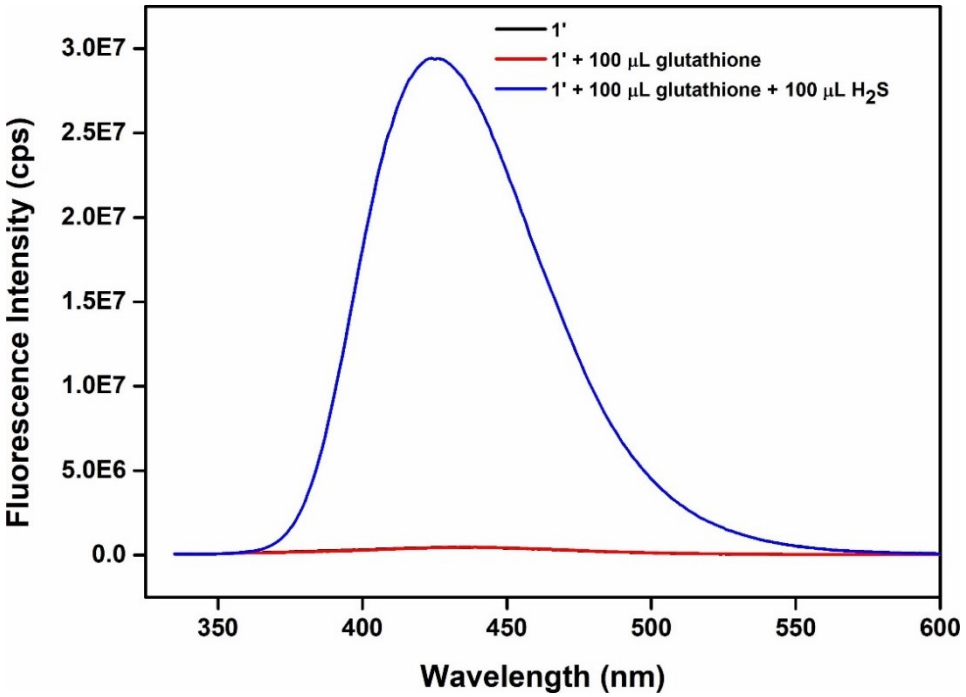

Figure S19. Switch-on fluorescence intensity of the aqueous solution of **1′** after addition of 100 μL of 10 mM aqueous Na_2S solution in presence of 100 μL of 10 mM aqueous solution of glutathione.

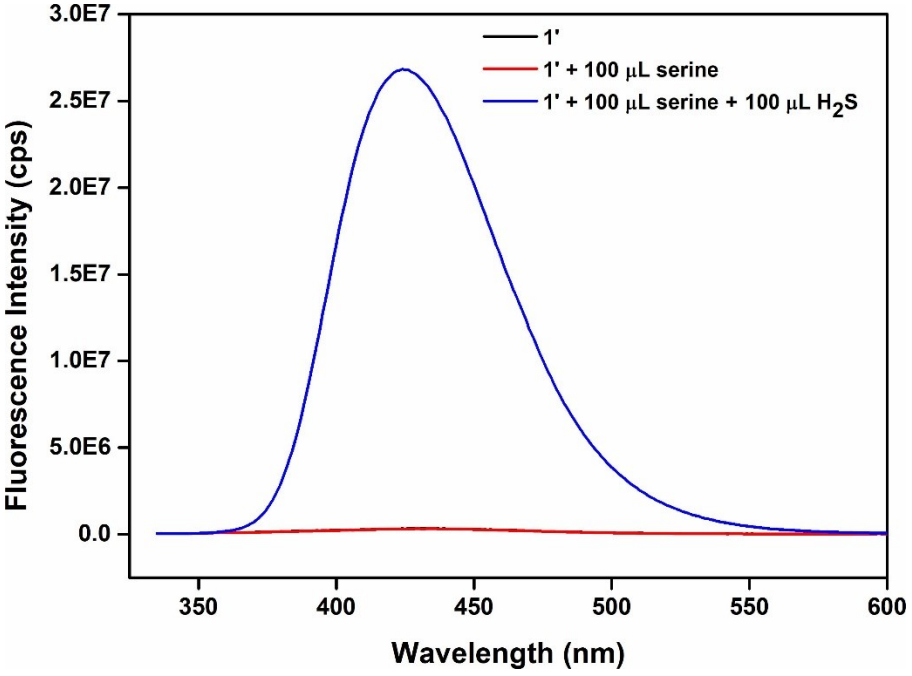

Figure S20. Switch-on fluorescence intensity of the aqueous solution of **1′** after addition of 100 μL of 10 mM aqueous Na_2S solution in presence of 100 μL of 10 mM aqueous solution of serine.

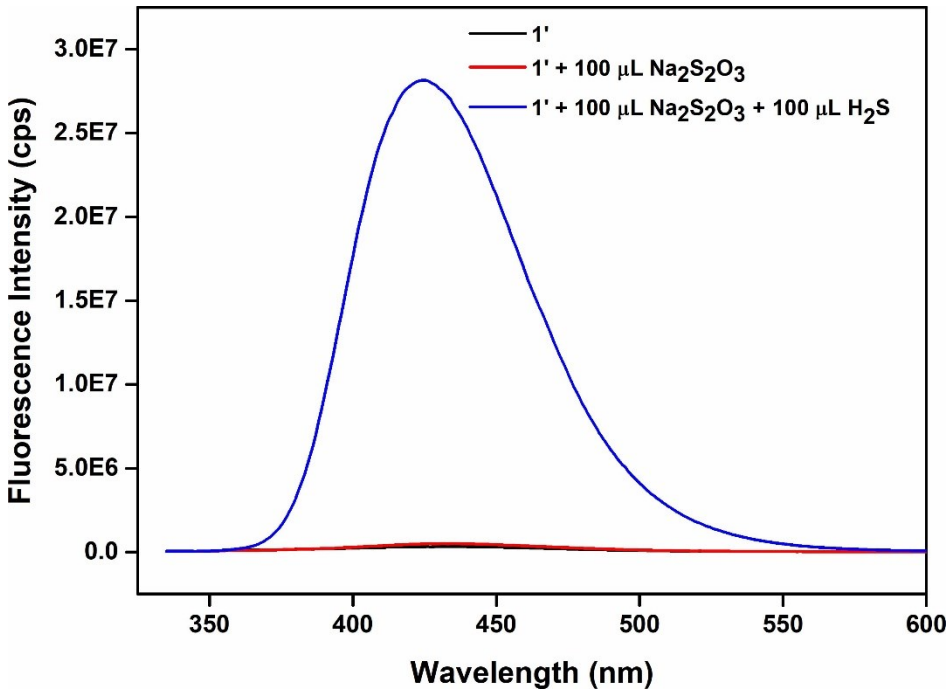

Figure S21. Switch-on fluorescence intensity of the aqueous solution of **1′** after addition of 100 μL of 10 mM aqueous Na_2S solution in presence of 100 μL of 10 mM aqueous solution of $Na_2S_2O_3$.

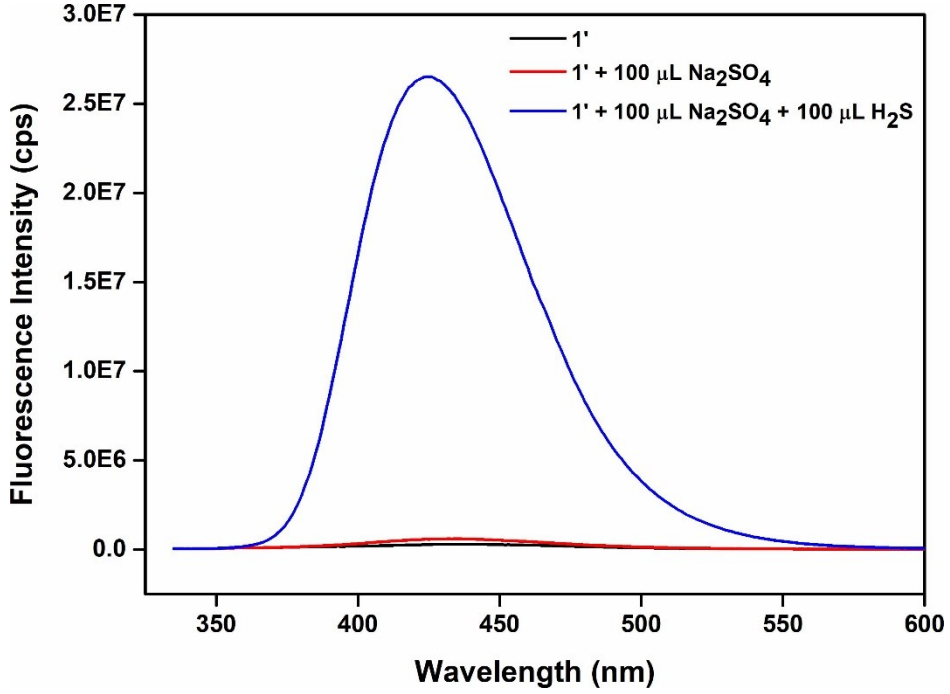

Figure S22. Switch-on of fluorescence intensity of the aqueous solution of **1′** after addition of 100 μL of 10 mM aqueous Na_2S solution in presence of 100 μL of 10 mM aqueous solution of Na_2SO_4.

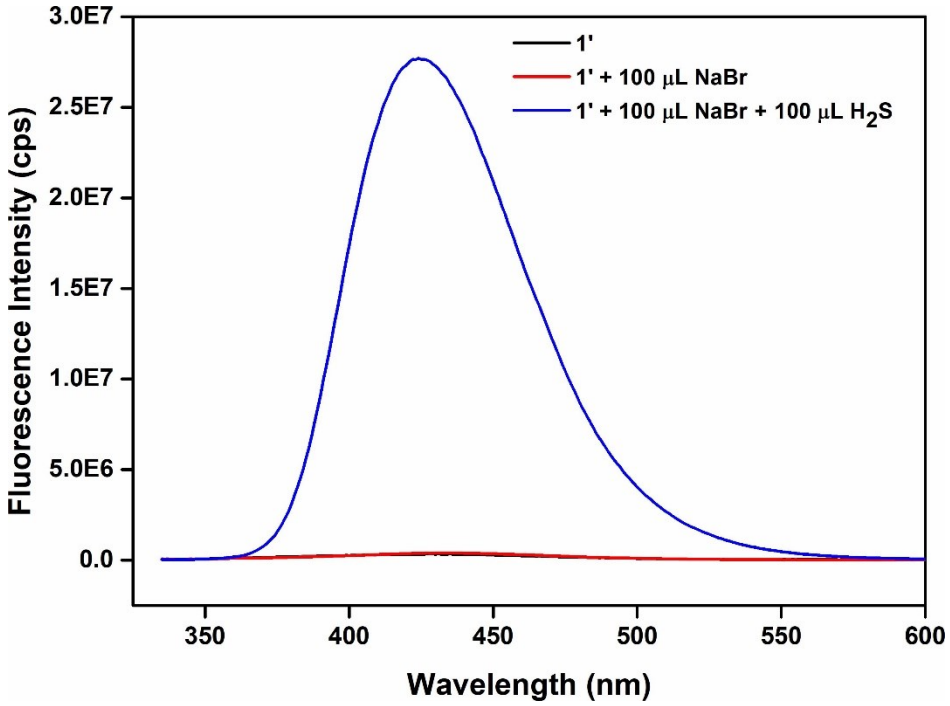

Figure S23. Switch-on fluorescence intensity of the aqueous solution of **1′** after addition of 100 μL of 10 mM aqueous Na_2S solution in presence of 100 μL of 10 mM aqueous solution of NaBr.

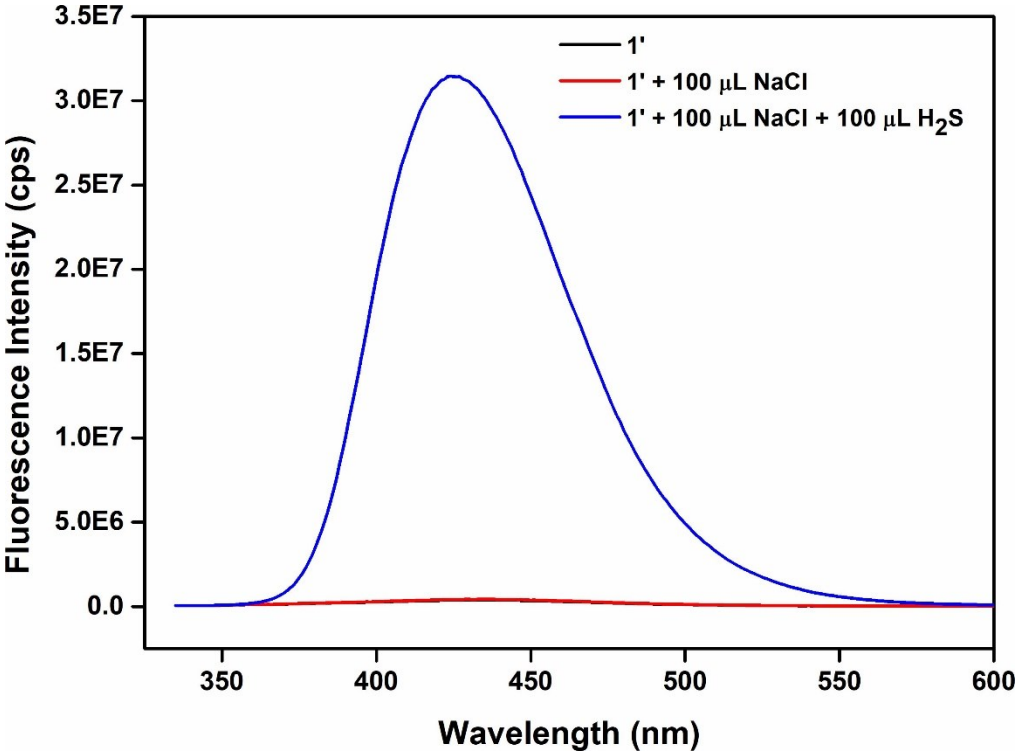

Figure S24. Switch-on fluorescence intensity of the aqueous solution of **1′** after addition of 100 μL of 10 mM aqueous Na_2S solution in presence of 100 μL of 10 mM aqueous solution of NaCl.

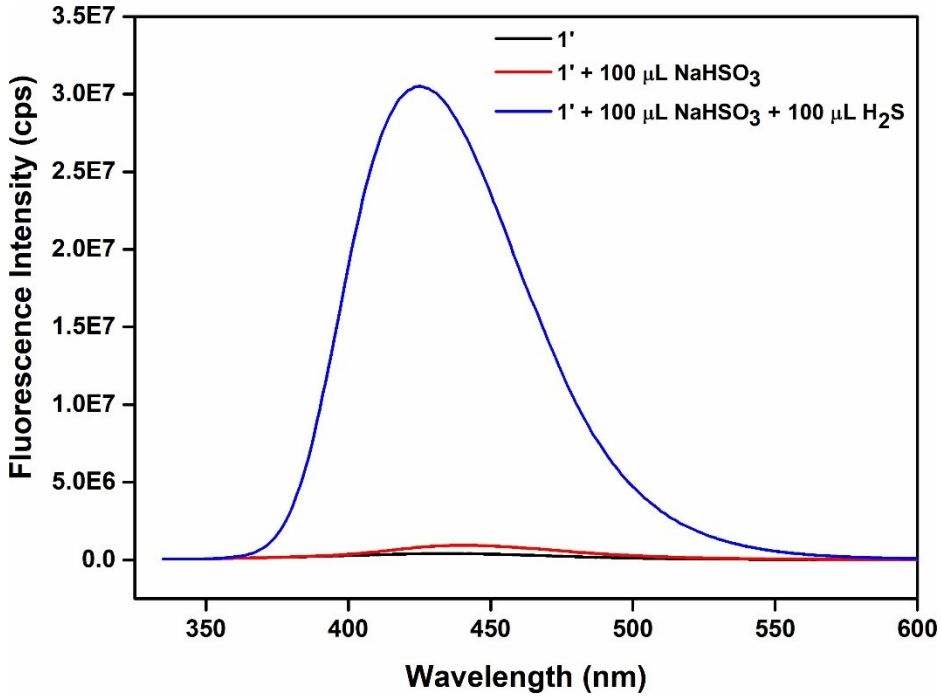

Figure S25. Switch-on fluorescence intensity of the aqueous solution of **1′** after addition of 100 μL of 10 mM aqueous Na_2S solution in presence of 100 μL of 10 mM aqueous solution of $NaHSO_3$.

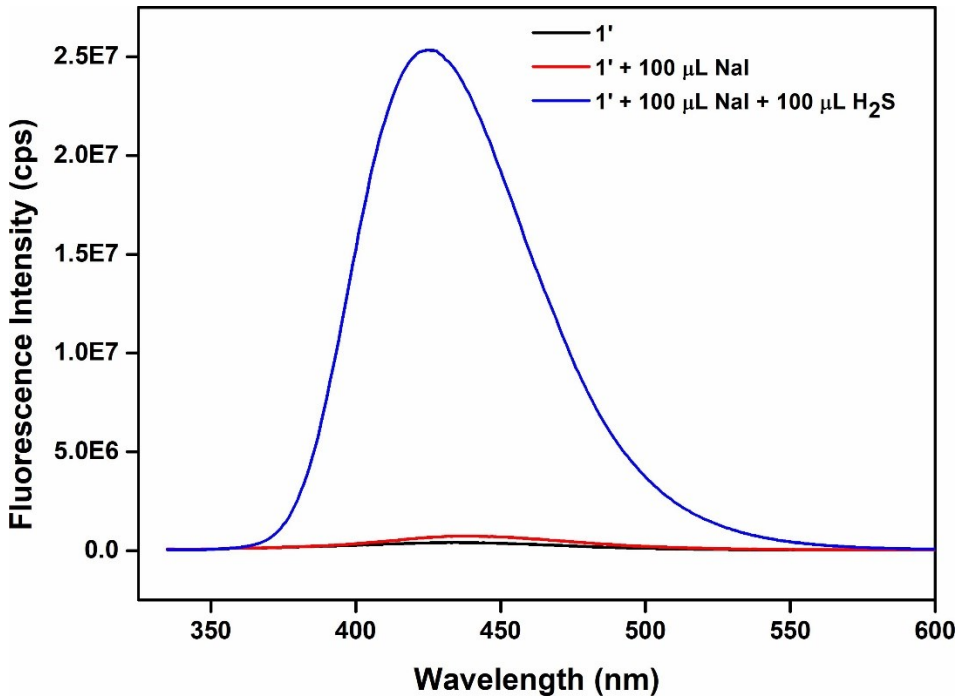

Figure S26. Switch-on fluorescence intensity of the aqueous solution of **1′** after addition of 100 μL of 10 mM aqueous Na_2S solution in presence of 100 μL of 10 mM aqueous solution of NaI.

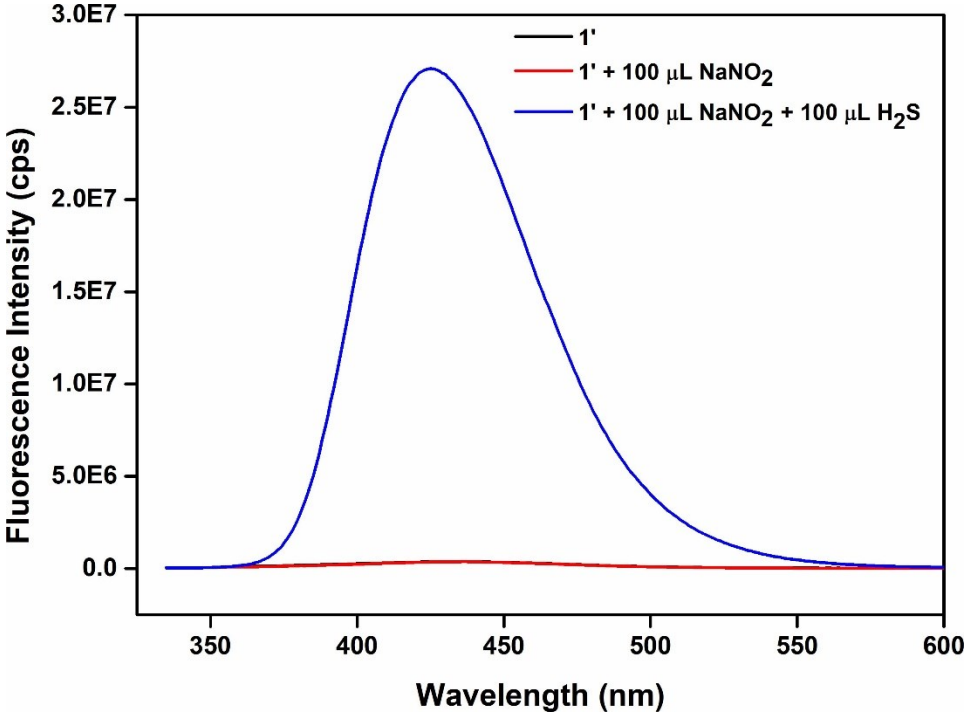

Figure S27. Switch-on fluorescence intensity of the aqueous solution of **1′** after addition of 100 μL of 10 mM aqueous Na_2S solution in presence of 100 μL of 10 mM aqueous solution of $NaNO_2$.

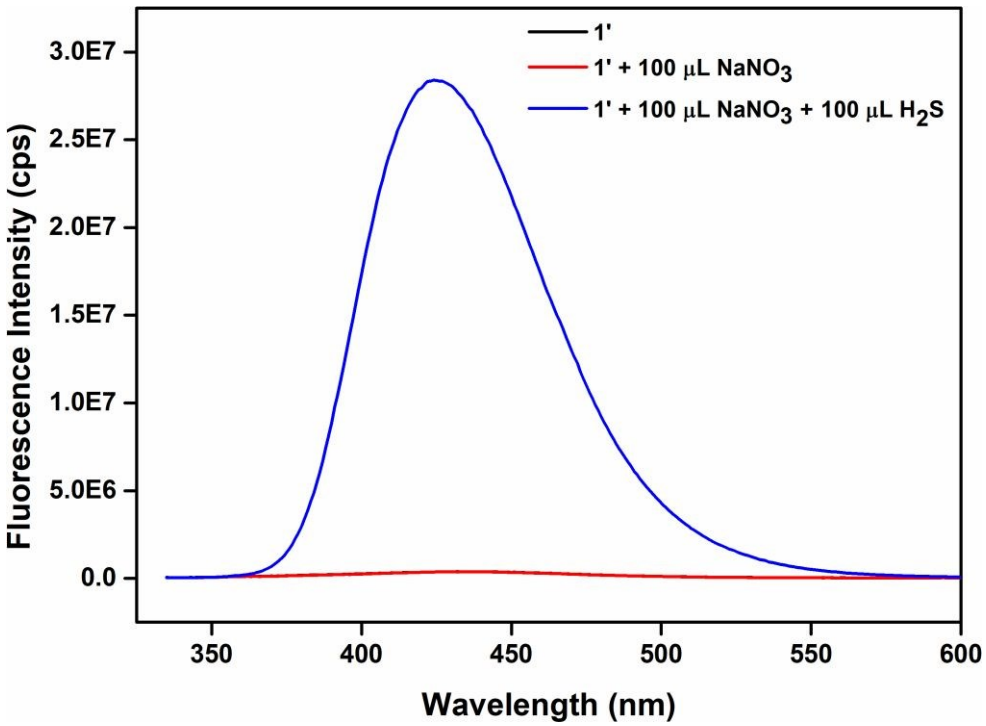

Figure S28. Switch-on fluorescence intensity of the aqueous solution of **1′** after addition of 100 μL of 10 mM aqueous Na_2S solution in presence of 100 μL of 10 mM aqueous solution of $NaNO_3$.

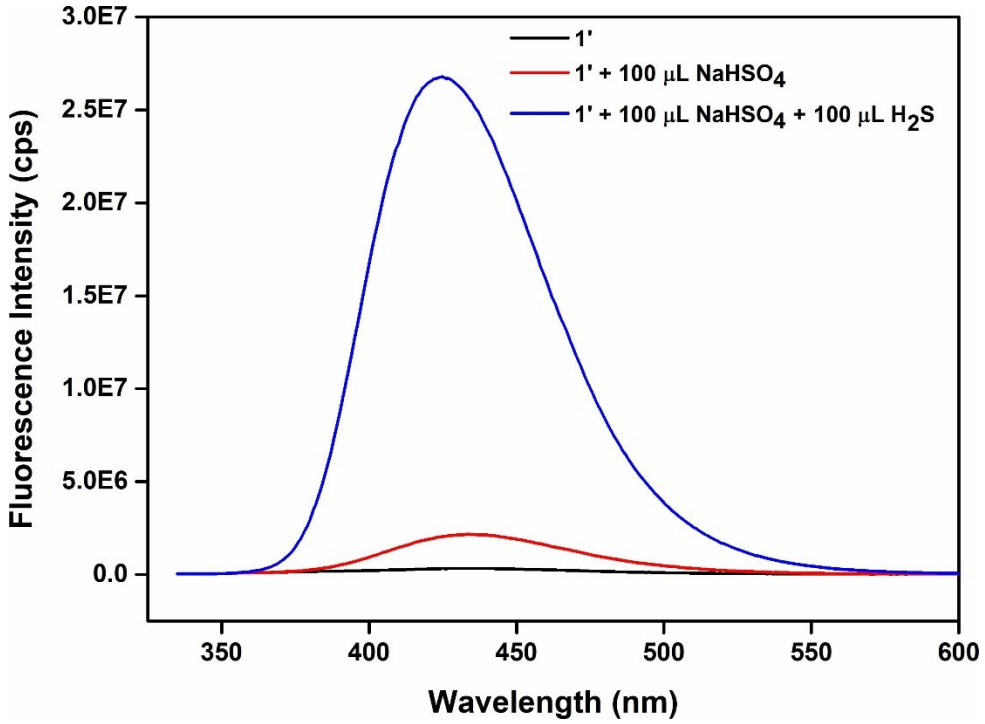

Figure S29. Switch-on fluorescence intensity of the aqueous solution of **1′** after addition of 100 μL of 10 mM aqueous Na_2S solution in presence of 100 μL of 10 mM aqueous solution of $NaHSO_4$.

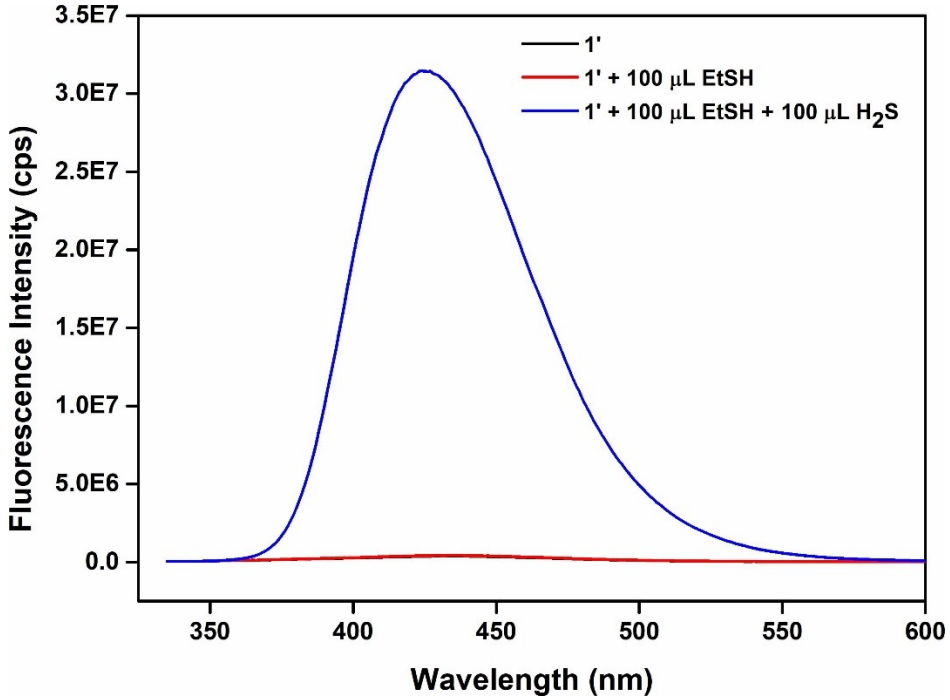

Figure S30. Switch-on fluorescence intensity of the aqueous solution of **1′** after addition of 100 μL of 10 mM aqueous Na_2S solution in presence of 100 μL of 10 mM aqueous solution of EtSH.

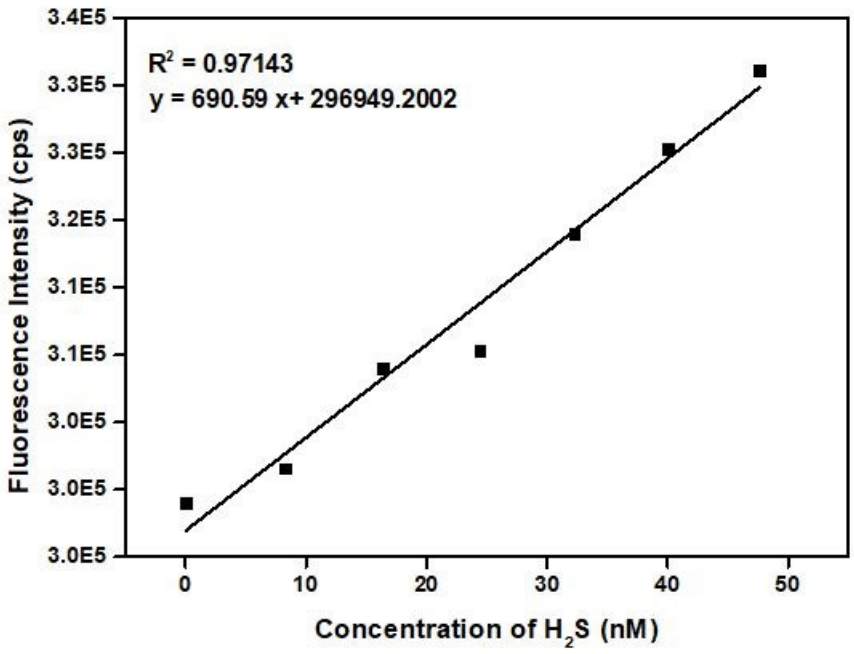

Figure S31. Change in the fluorescence intensity of **1′** in HEPES buffer as a function of H_2S concentration.

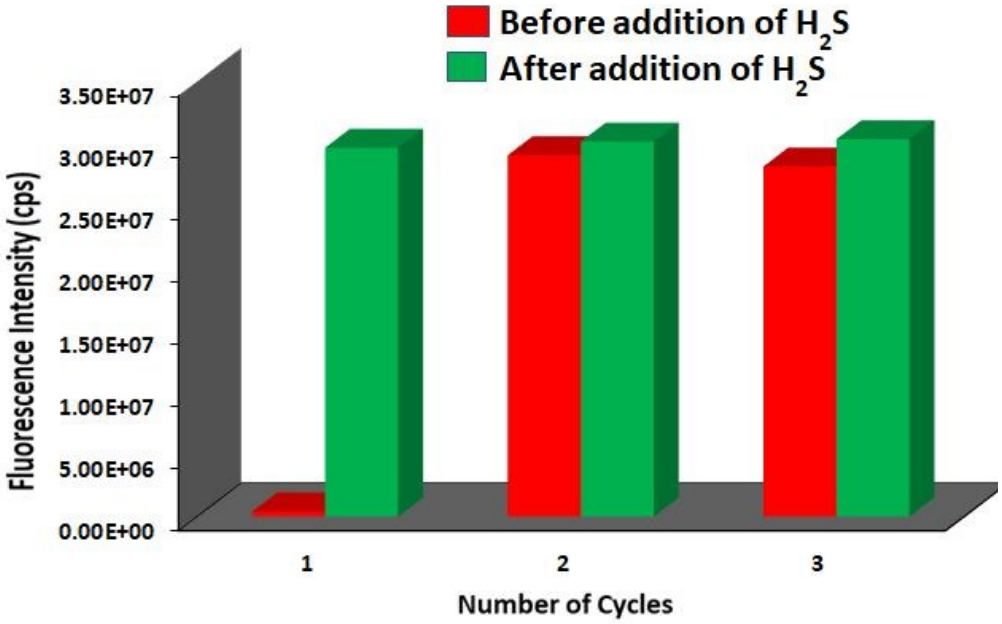

Figure S32. Recyclability plot of **1′** towards the sensing of H_2S in aqueous medium.

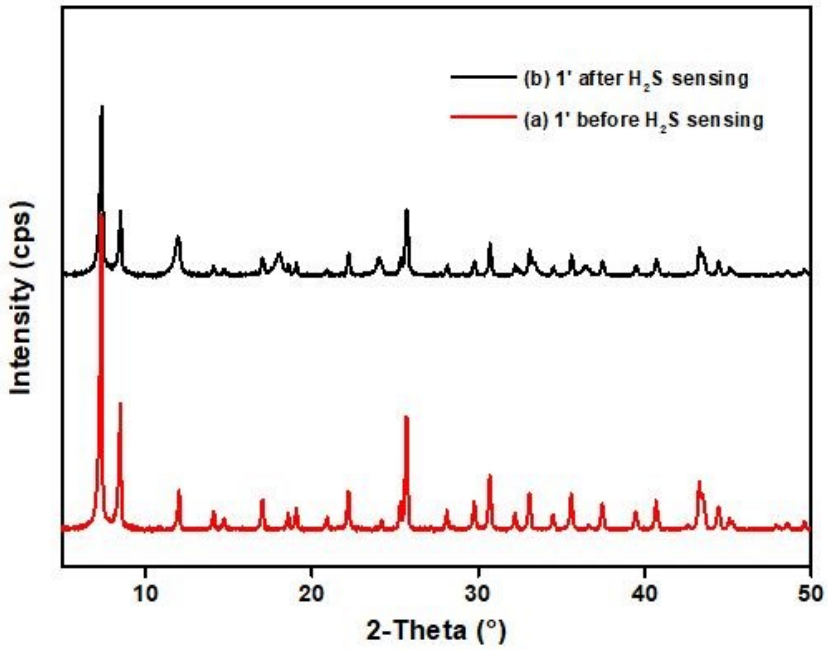

Figure S33. PXRD patterns of compound **1′** (a) after and (b) before treatment with H_2S in aqueous medium.

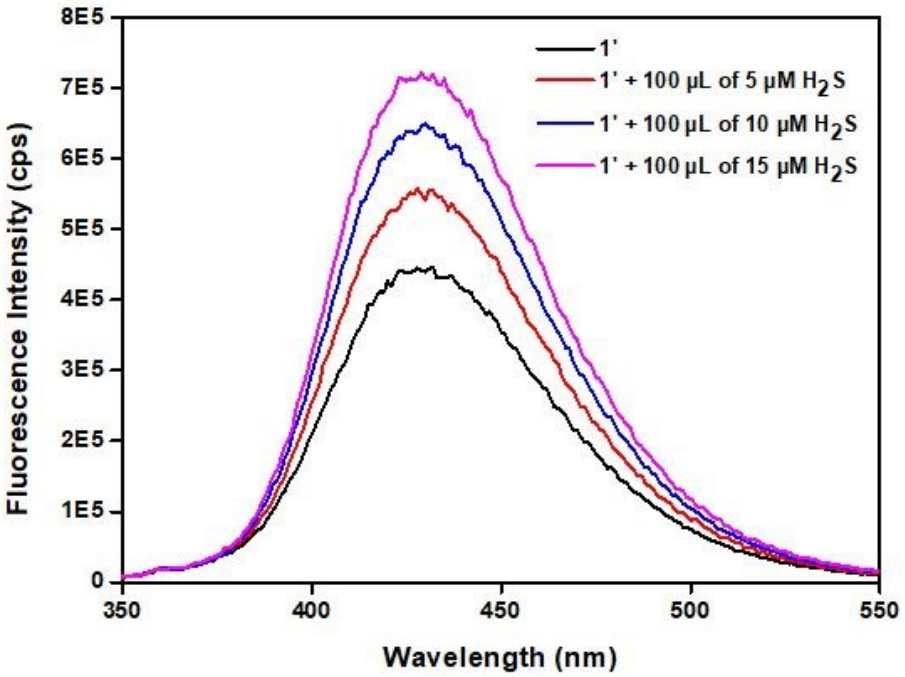

Figure S34. Switch-on fluorescence intensity of the distilled water suspension of **1′** after addition of 100 µL of 5, 10 and 15 µM Na_2S solution in distilled water.

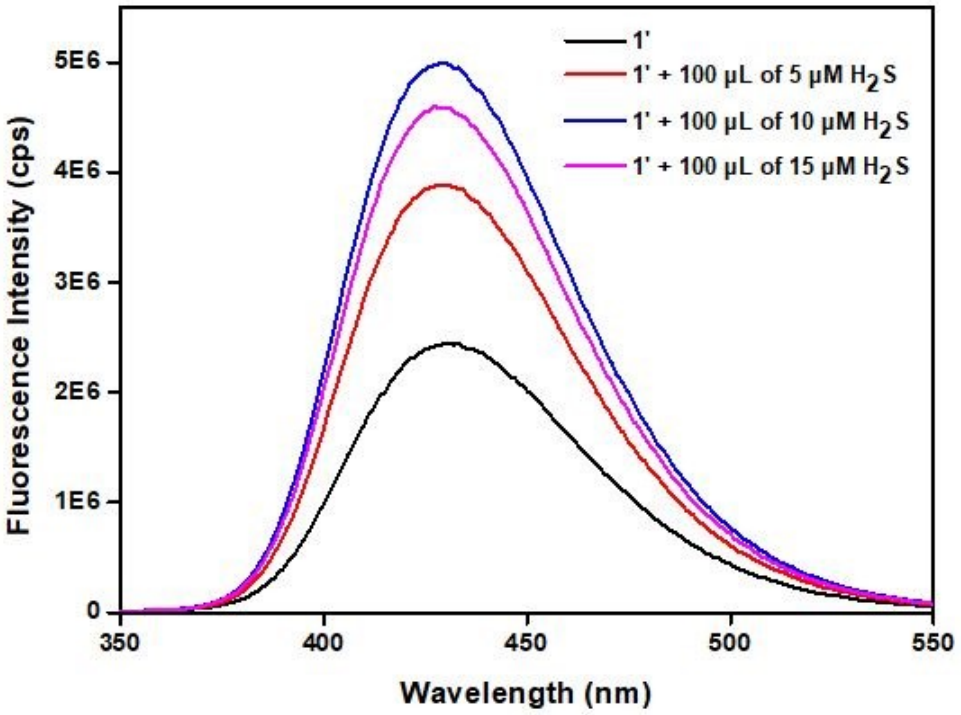

Figure S35. Switch-on fluorescence intensity of the tap water suspension of **1′** after addition of 100 µL of 5, 10 and 15 µM Na_2S solution in tap water.

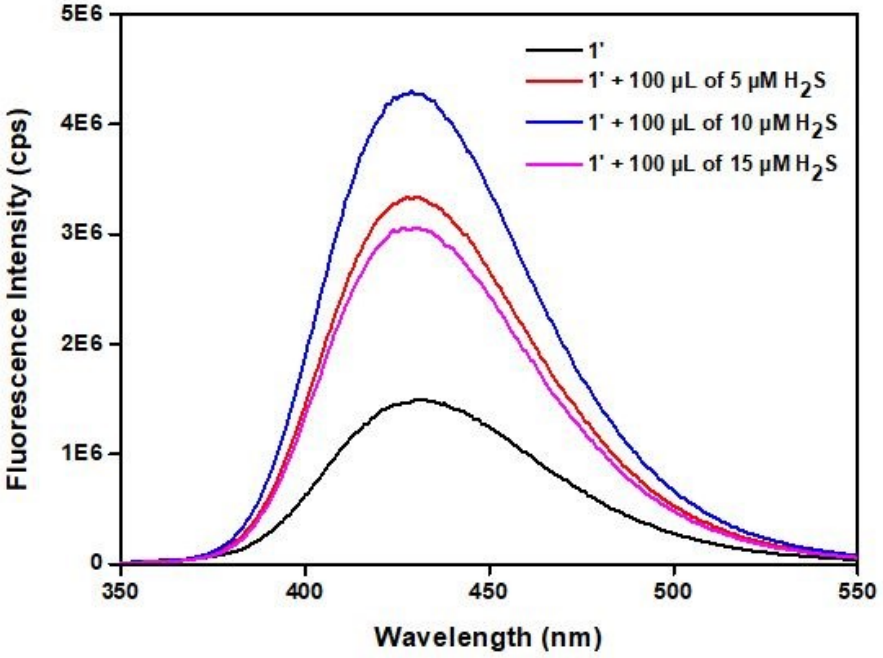

Figure S36. Switch-on fluorescence intensity of the river water suspension of **1′** after addition of 100 µL of 5, 10 and 15 µM Na_2S solution in river water.

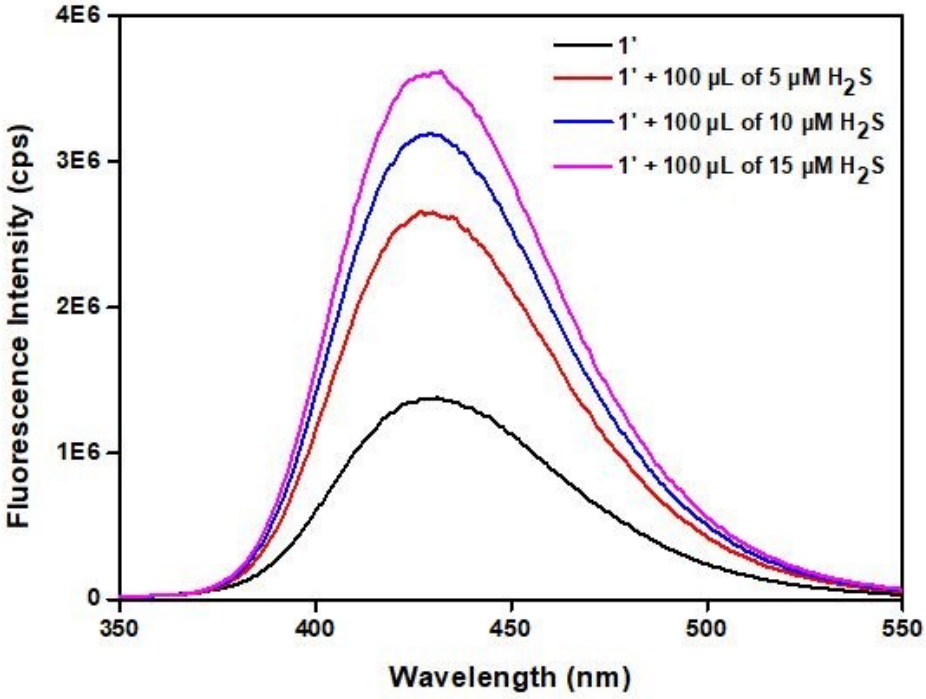

Figure S37. Switch-on fluorescence intensity of the lake water suspension of **1′** after addition of 100 µL of 5, 10 and 15 µM Na_2S solution in lake water.

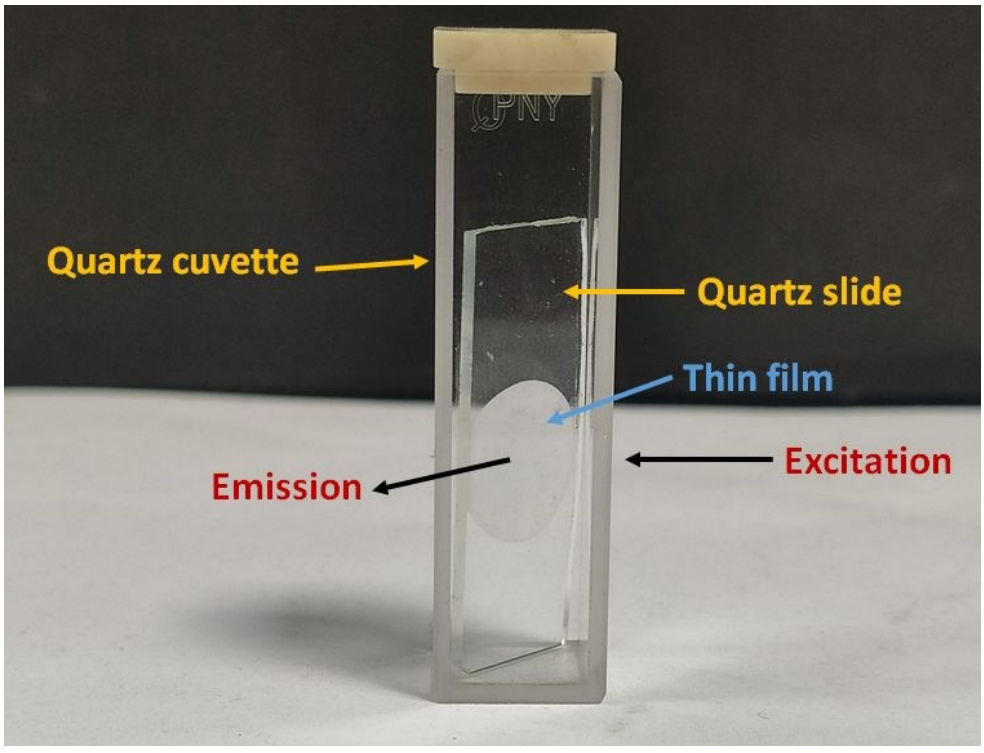

Figure S38. Image of the set-up used for the H_2S sensing in gas phase.

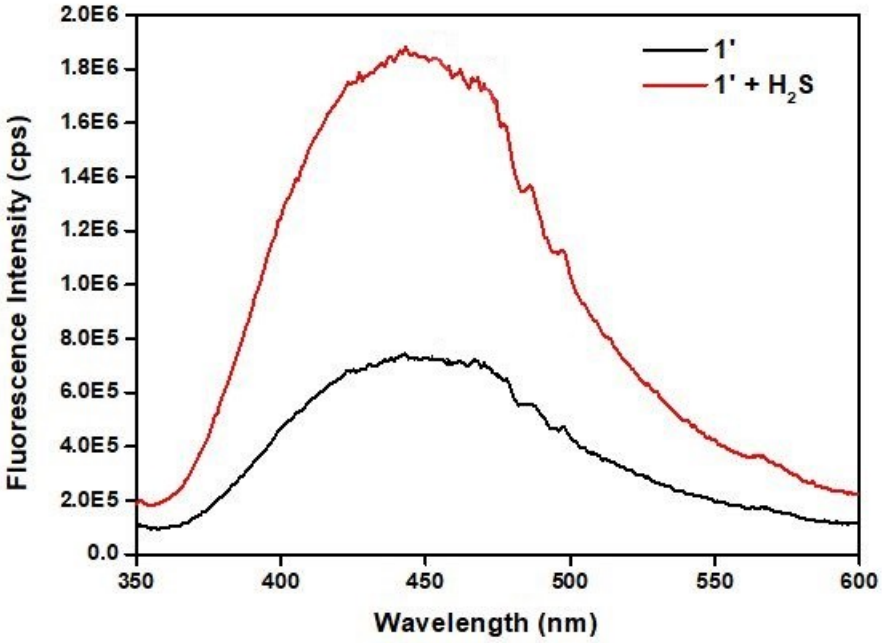

Figure S39. Switch-on fluorescence intensity of the aqueous solution of **1′** upon exposure to H_2S gas for 6 min. 25 mg of solid Na_2S was added to 1 mL of 6 (M) HCl solution inside the quartz cuvette to generate H_2S gas.

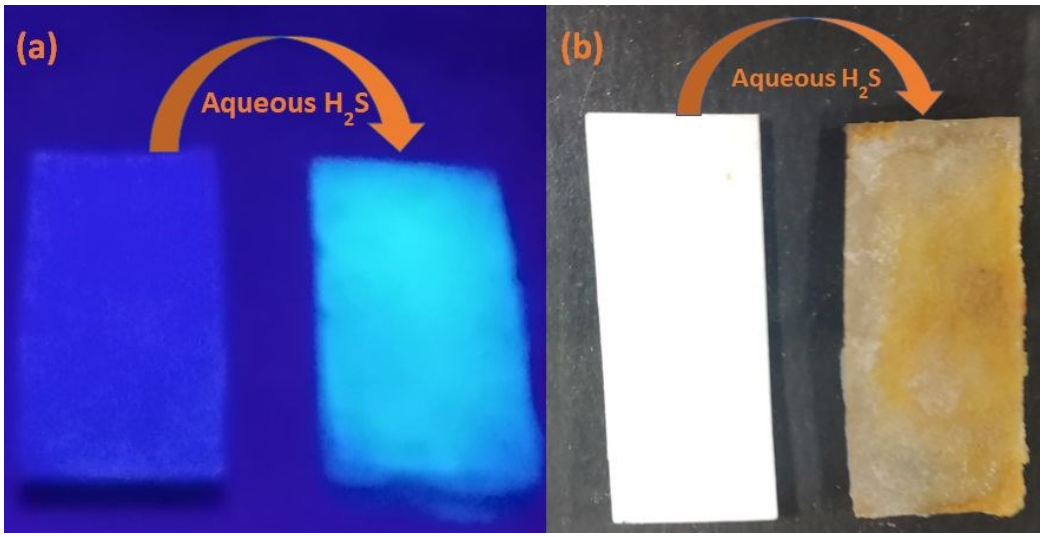

Figure S40. Images of **1′**-coated paper strips (a) under UV lamp and (b) in day light after treating with 10 mM aqueous Na_2S solution.

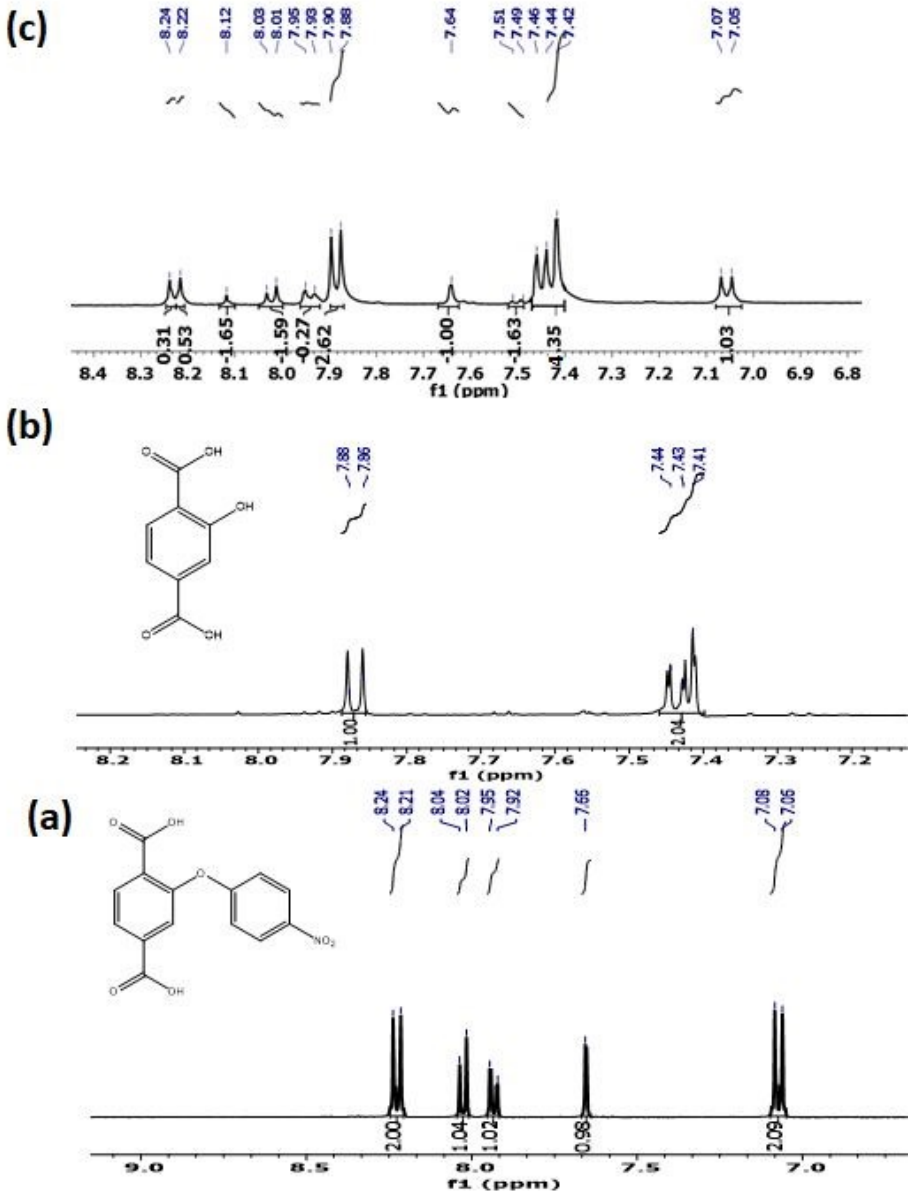

Figure S41. ^{1}H NMR spectra of (a) H_2BDC-O-Ph-NO_2 linker, (b) free H_2BDC-OH and (c) **1′** after treatment with Na_2S, followed by digestion with two drops of 40% HF in DMSO-d_6. After comparing these three spectra, we can conclude that after treatment with Na_2S, the BDC-O-Ph-NO_2 linker in **1′** is partially fragmented into BDC-OH and HS-Ph-NO_2. The two new peaks at 8.12 and 7.51 ppm are due to the presence of free HS-Ph-NO_2. The new peaks at 7.88, 7.46,7.44 and 7.42 confirm the presence of free H_2BDC-OH. The percentage of fragmentation can be calculated from the integral values obtained for the two newly generated peaks, which correspond to the HS-Ph-NO_2 molecule. The percentage of fragmentation of the BDC-O-Ph-NO_2 linker in **1′** into BDC-OH and HS-Ph-NO_2 was calculated to be ~82%.

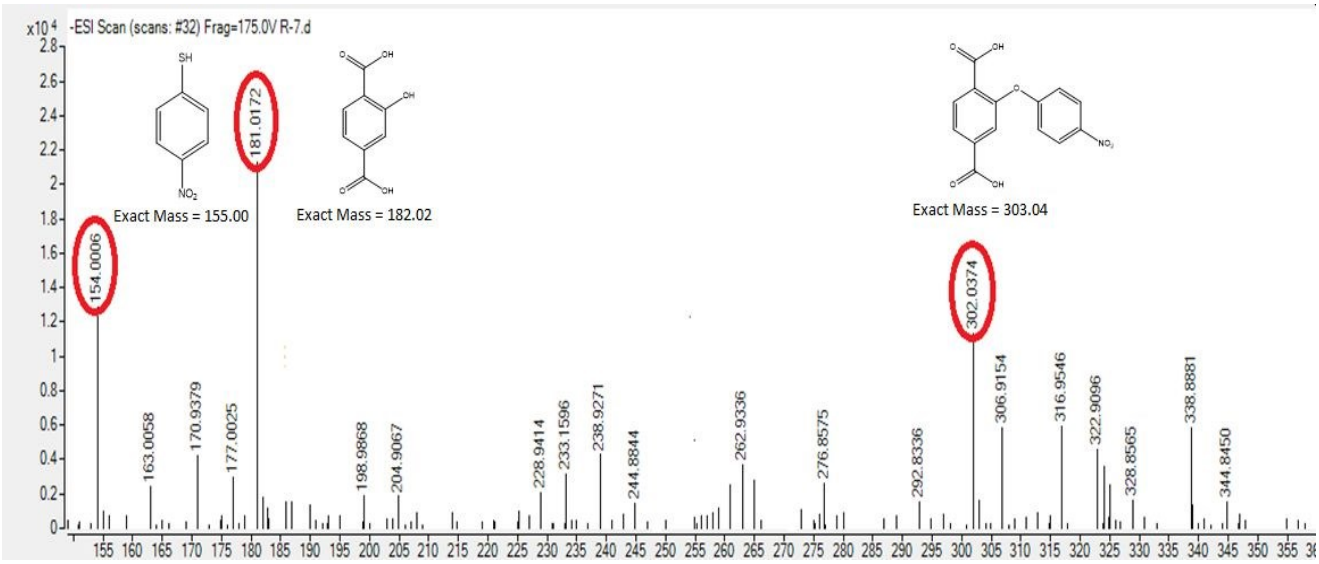

Figure S42. ESI-MS spectrum of Na_2S-treated **1′** (digested in MeOH/HF) showing m/z (negative ion mode) peaks at 154.0006, 181.0172, and 302.0374 which correspond to $(M-H)^-$ ion of HS-Ph-NO_2, H_2BDC-OH and H_2BDC-O-Ph-NO_2 linker respectively.

Table S1. Unit cell parameters of the as-synthesized Zr-UiO-66-O-Ph-NO_2 MOF. The obtained values are compared with the un-functionalized Zr-UiO-66 MOF.

Compound Name	Zr-UiO-66-O-Ph-NO_2 (this work)	Zr-UiO-66 MOF (reported)[1]
Crystal System	cubic	cubic
a = b = c (Å)	20.774 (4)	20.7004(2)
α = β= γ (°)	90	90
V (Å^3)	8965.2 (32)	8870.3(2)

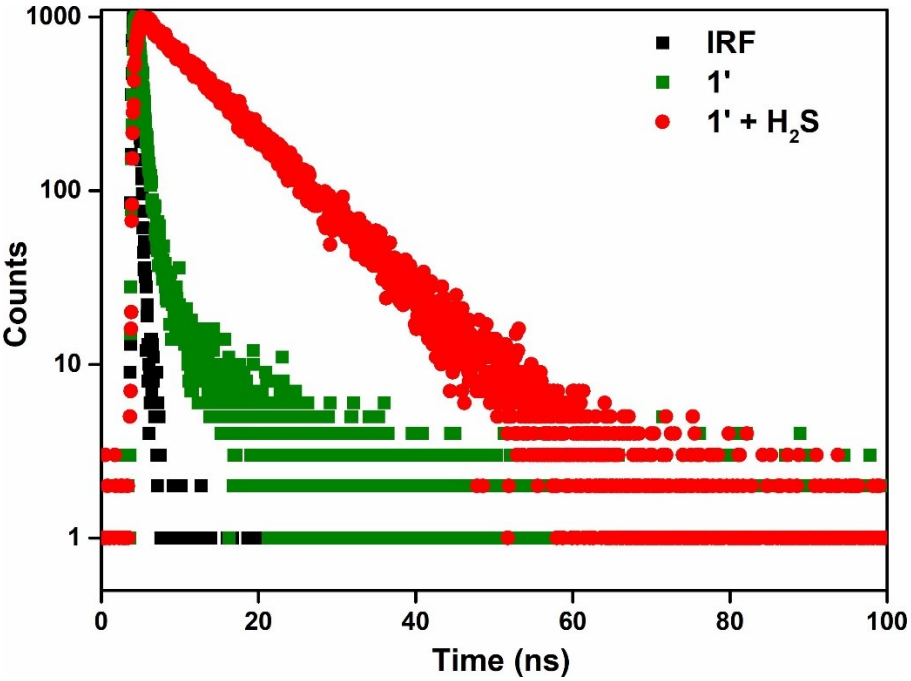

Figure S43. Lifetime decay profile of **1′** in absence and presence of aqueous solution of Na_2S (λ_{ex} = 320 nm, monitored at 308 nm).

Table S2. Fluorescence lifetimes of **1′** before and after the addition of 10 mM Na_2S solution (λ_{ex} = 320 nm, 308 nm pulsed diode laser).

Volume of Na_2S solution added (μL)	a_1	a_2	τ_1 (ns)	τ_2 (ns)	$\langle\tau\rangle$* (ns)
0	0.78	0.22	0.74	6.39	1.98
100	0.06	0.94	1.46	9.94	9.43

* $\langle\tau\rangle = a_1\tau_1 + a_2\tau_2$

Table S3. Comparison of the response time, detection limit and analyte used for the reported chemosensors of H_2S in the literature

Sl. No.	Sensor Material	Type of Material	Method Used	Response Time (s)	Detection Limit	Analyte Used	Ref.
1	cpGFP-Tyr66pAzF	Organic molecule	Fluorescence	420	-	NaSH	2
2	CTN	Organic molecule	Fluorescence	-	90 nM	NaSH	3
3	DNS-Az	Organic molecule	Fluorescence	-	1 μM	Na_2S	4
4	SF4	Organic molecule	Fluorescence	-	0.125 μM	NaSH	5
5	π-conjugation rhodamine-NBD	Organic molecule	Fluorescence	-	0.37 μM	Na_2S	6
6	PSS-PA-Cu NC aggregates	Nano cluster aggregates	Fluorescence	-	0.65 μM	Na_2S	7
7	bare gold NPs	Nanoparticles	UV-vis spectroscopy	-	0.08 μM	Na_2S	8
8	CuO-BSST	Semi conducting oxide	Conductivity impedance	10	4-10 ppb	H_2S	9
9	ZnO rod	Conductivity impedance	Conductivity impedance	-	50 ppb	H_2S	10
10	nafion membrane (H_2SO_4 treated)	Amperometry	Amperometry	9	100 ppb	H_2S	11
11	In_2O_3 whiskers	Semi conducting oxide	Conductivity impedance	120-210	200 ppb	H_2S	12
12	polymer P1	Semiconducting polymer	Conductivity impedance	-	1 ppb	H_2S	13
13	polyaniline nanowires-gold nanoparticles	Conducting polymer	Conductivity impedance	<120	0.1 ppb	H_2S	14

14	probe 1	Organic molecule	Fluorescence	3600	2.4 μM	NaSH	15
15	QCM coated with PPy/TiO_2 film	Quartz-crystal microbalance	Frequency shift	-	10 ppm	H_2S	16
16	WSP5	Organic molecule	Fluorescence	-	0.047 μM	NaSH	17
17	SFP-1 SFP-1	Organic molecule	Fluorescence	7200 14400	- -	H_2S	18
18	NHS1	Organic molecule	Fluorescence	4800	0.02 μM	NaHS	19
19	Cy-N_3	Organic molecule	Fluorescence	1200	0.08 μM	NaHS	20
20	SHS-M1 SHS-M2	Organic molecule	Fluorescence	- -	0.2 μM 0.4 μM	Na_2S	21
21	CAU-10-V-H	MOF	Fluorescence	10	1.65 μM	NaHS	22
22	UiO-66-CH=CH_2	MOF	Fluorescence	10	6.46 μM	NaHS	23
23	Al-TCPP-Cu	MOF	Fluorescence	-	-	-	24
25	Al-MIL-101-N_3	MOF	Fluorescence	-	100 μM	Na_2S	25
26	MN-ZIF-90	MOF	Fluorescence	510	25 μM	H_2S	26
27	$[CuL(AlOH)_2]_n$	MOF	Fluorescence	360	0.02 μM	NaHS	27
28	$[EuCu(pydc)_2(ox)_{0.5}(H_2O)_3 \cdot 1.5H_2O]_{2n}$	MOF	Fluorescence	120	0.13 μM	H_2S	28
29	Tb^{3+}@Cu-MOF	MOF	Fluorescence	120	1.2 μM	Na_2S	29
30	Zr-UiO-66-$(NO_2)_2$	MOF	Fluorescence	2400	14.14 μM	Na_2S	30
31	Al-MIL-53-N_3	MOF	Fluorescence	180	0.09 μM	Na_2S	31
32	IRMOF-3-N_3	MOF	Fluorescence	<120	24.3 μM	Na_2S	32

33	Zr-UiO-66-NO_2	MOF	Fluorescence	460	188 μM	Na_2S	33
34	Ce-UiO-66-N_3	MOF	Fluorescence	760	12.2 μM	NaHS	34
35	DUT-52-$(NO_2)_2$	MOF	Fluorescence	3300	20 μM	Na_2S	35
36	Ce-UiO-66-NO_2	MOF	Fluorescence	760	34.84 μM	NaHS	34
37	CAU-10-N_3	MOF	Fluorescence	420	2.65 μM	Na_2S	36
38	Zr-UiO-66-N_3	MOF	Fluorescence	180	118 μM	Na_2S	37
39	Eu^{3+}/Cu^{2+}@UiO-66-$(COOH)_2$	MOF	Fluorescence	30	5.45 μM	NaHS	38
40	DUT-52-N_3	MOF	Fluorescence	120	0.50 μM	Na_2S	39
41	Fe^{III}-MIL-88-NH_2	MOF	Fluorescence	300	10 μM	NaHS	40
42	$[Zr_6O_4(OH)_4(BDC\text{-}C_6H_4NO_3)_6]\cdot 6H_2O\cdot$ 7DMF	MOF	Fluorescence	60	12.58 nM	Na_2S	this work

References:

1. J. H. Cavka, S. Jakobsen, U. Olsbye, N. Guillou, C. Lamberti, S. Bordiga and K. P. Lillerud, *J. Am. Chem. Soc.*, 2008, 42, 13850–13851.
2. S. Chen, Z.-j. Chen, W. Ren and H.-w. Ai, *J. Am. Chem. Soc.*, 2012, 134, 9589–9592.
3. J. Cui, T. Zhang, Y.-Q. Sun, D.-P. Li, J.-T. Liu and B.-X. Zhao, *Sens. Actuators. B*, 2016, 232, 705-711.
4. H. Peng, Y. Cheng, C. Dai, A. L. King, B. L. Predmore, D. J. Leferand and B. Wang, *Angew. Chem. Int. Ed.*, 2011, 50, 9672-9675.
5. V. S. Lin, A. R. Lippert and C. J. Chang, *Proc. Natl. Acad. Sci. U. S. A.*, 2013, 110, 7131-7135.
6. I. Ismail, Z. Chen, X. Ji, L. Sun, L. Yi and Z. Xi, *Molecules*, 2020, 25, 437=442.
7. P.-C. Chen, Y.-C. Li, J.-Y. Ma, J.-Y. Huang, C.-F. Chen and H.-T. Chang, *Sci. Rep.*, 2016, 6, 24882-24890.
8. H.-H. Deng, S.-H. Weng, S.-L. Huang, L.-N. Zhang, A.-L. Liu, X.-H. Lin and W. Chen, *Anal. Chim. Acta*, 2014, 852, 218-222.
9. G. H. Jain and L. A. Patil, *Sens. Actuators B Chem.*, 2007, 123, 246-253.
10. C. Wang, X. Chu and M. Wu, *Sens. Actuators B Chem.*, 2006, 113, 320-323.
11. C. Yu, Y. Wang, K. Hua, W. Xing and T. Lu, *Sens. Actuators B Chem.*, 2002, 96, 259-265.
12. M. Kaur, N. Jain, K. Sharma, S. Bhattacharya, M. Roy, A. K. Tyagi, S. K. Gupta and J. V. Yakhmi, *Sens. Actuators B Chem.*, 2008, 133, 456-461.
13. A. Lv, M. Wang, Y. Wang, Z. Bo and L. Chi, *Chem. Eur .J.*, 2016, 22, 3654-3659.

14. M. D. Shirsat, M. A. Bangar, M. A. Deshusses, N. V. Myung and A. Mulchandani, *Appl. Phys. Lett.*, 2009, 94, 083502-083504.
15. Y. Jiang, Q. Wu and X. Chang, *Talanta*, 2014, 121, 122-126.
16. S. Cui, L. Yang, J. Wang and X. Wang, *Sens. Actuators B Chem.*, 2016, 233, 337-346.
17. B. Peng, W. Chen, C. Liu, E. W. Rosser, A. Pacheco, Y. Zhao, H. C. Aguilar and M. Xian, *Chem. Eur. J.*, 2014, 20, 1010-1016.
18. Y. Qian, J. Karpus, O. Kabil, S.-Y. Zhang, H.-L. Zhu, R. Banerjee, J. Zhao and C. He, *Nat. Commun.*, 2011, 2, 495-501.
19. G.-J. Mao, T.-T. Wei, X.-X. Wang, S. Huan, D.-Q. Lu, J. Zhang, X.-B. Zhang, W. Tan, G.-L. Shen and R.-Q. Yu, *Anal. Chem.*, 2013, 85, 7875-7881.
20. F. Yu, P. Li, P. Song, B. Wang, J. Zhao and K. Han, *Chem. Commun.*, 2012, 48, 2852-2854.
21. S. K. Bae, C. H. Heo, D. J. Choi, D. Sen, E.-H. Joe, B. R. Cho and H. M. Kim, *J. Am. Chem. Soc.*, 2013, 135, 9915-9923.
22. Y. Li, X. Zhang, L. Zhang, K. Jiang, Y. Cui, Y. Yang and G. Qian, *J. Solid State Chem.*, 2017, 255, 97-101.
23. S. Nandi, H. Reinsch and S. Biswas, *Microporous and Mesoporous Mater.*, 2020, 293, 109790-109798.
24. Y. Ma, H. Su, X. Kuang, X. Li, T. Zhang and B. Tang, *Anal. Chem.*, 2014, 86, 11459-11463.
25. A. Legrand, A. Pastushenko, V. Lysenko, A. Geloen, E. A. Quadrelli, J. Canivet and D. Farrusseng, *ChemNanoMat*, 2016, 2, 866-872.
26. H. Li, X. Feng, Y. Guo, D. Chen, R. Li, X. Ren, X. Jiang, Y. Dong and B. Wang, *Sci. Rep.*, 2014, 4, 4366-4370.
27. Y. Ma, H. Su, X. Kuang, X. Li and T. Zhang, *B. Tang, Anal. Chem.*, 2014, 86, 11459-11463.
28. X. Zhang, J. Zhang, Q. Hu, Y. Cui, Y. Yang and G. Qian, *Appl. Surf. Sci.*, 2015, 355, 814-819.
29. X. Zheng, R. Fan, Y. Song, A. Wang, K. Xing, X. Du, P. Wang and Y. Yang., *J. Mater. Chem. C*, 2017, 5, 9943-9951.
30. S. Nandi, S. Banesh, V. Trivedi and S. Biswas, *Analyst*, 2018, 143, 1482-1491.
31. A. Das, S. Banesh, V. Trivedi and S. Biswas, *Dalton Trans.*, 2018, 47, 2690-2700.
32. X. Zheng, R. Fan, Y. Song, K. Xing, P. Wang and Y. Yang, *ACS Appl. Mater. Interfaces*, 2018, 10, 32698-32706.
33. S. S. Nagarkar, A. V. Desai and S. K. Ghosh, *Chem. Eur. J.*, 2015, 21, 9994-9997.
34. A. Buragohain and S. Biswas, *CrystEngComm*, 2016, 18, 4374-4381.
35. R. Dalapati, S. N. Balaji, V. Trivedi, L. Khamari and S. Biswas, *Sens. Actuators. B*, 2017, 245, 1039-1049.
36. S. Nandi, H. Reinsch, S. Banesh, N. Stock, V. Trivedi and S. Biswas, *Dalton Trans.*, 2017, 46, 12856-12864.
37. S. S. Nagarkar, T. Saha, A. V. Desai, P. Talukdar and S. K. Ghosh, *Sci. Rep.*, 2014, 4, 7053-7058.
38. X. Zhang, Q. Hu, T. Xia, J. Zhang, Y. Yang, Y. Cui, B. Chen and G. Qian, *ACS Appl. Mater. Interfaces*, 2016, 8, 32259-32265.
39. C. Gogoi, A. Kumar and M. SK, *Microporous Mesoporous Mater.*, 2021, 311, 110725-110731.
40. Y.-Y. Cao, X.-F. Guo and H. Wang, *Sens. Actuators B Chem.*, 2017, 243, 8-17.